

Computing Robust Forward Invariant Sets of Multidimensional Non-linear Systems via Geometric Deformation of Polytopes

Taha Ameen, Shayok Mukhopadhyay, and Nasser Qaddoumi

Abstract—This paper develops and implements an algorithm to compute sequences of polytopic Robust Forward Invariant Sets (RFIS) that can parametrically vary in size between the maximal and minimal RFIS of a nonlinear dynamical system. This is done through a novel computational approach that geometrically deforms a polytope into an invariant set using a sequence of homeomorphisms, based on an invariance condition that only needs to be satisfied at a finite set of test points. For achieving this, a fast computational test is developed to establish if a given polytopic set is an RFIS. The geometric nature of the proposed approach makes it applicable for arbitrary Lipschitz continuous nonlinear systems in the presence of bounded additive disturbances. The versatility of the proposed approach is presented through simulation results on a variety of nonlinear dynamical systems in two and three dimensions, for which, sequences of invariant sets are computed.

Index Terms—Invariant Sets, Robust Forward Invariance, Nonlinear dynamical systems, Computational Topology.

I. INTRODUCTION

A Forward Invariant Set (FIS) for a dynamical system is a subset of the state space, from which state vector trajectories never escape as time runs forward. Invariant sets are fundamental objects in dynamical systems, and find applications in reachability analysis, as well as characterization of system stability and robustness. The latter is particularly useful in applications with strict performance and safety requirements, as the FIS provides bounds on system states. This is more valuable when such bounds can be guaranteed in the presence of disturbances through finding Robust Forward Invariant Sets (RFIS) for the system. Because any system trajectory that begins in an FIS stays in it, finding an invariant set that is disjoint from an unsafe set of states can ensure that system trajectories never reach an undesirable subset of the state space, if the initial conditions are picked to start within such a computed FIS. Further, an RFIS of the appropriate size can guarantee safety and robustness without imposing over-conservative or over-aggressive bounds on system trajectories. Thus motivated, this work focuses on computing RFISs in an n -dimensional setting. The two extremes, which are useful for performance analysis and controller synthesis [1], are the minimal RFIS, \mathcal{R}_s and the maximal RFIS \mathcal{R}_m .

Invariant sets also find application in Model Predictive Control (MPC), where they are used as target sets, and

can be used to provide domains of attraction for MPC-based controllers [2]. Of special interest are polytopic FIS, which guarantee stability without compromising any loss of performance [3], [4]. It is therefore no surprise that the characterization and computation of robust forward invariant sets for various systems is an active area of research, as seen in the following review of literature.

Traditional approaches for computing estimates of the invariant set include Carleman Linearizations [5] and PDE-based approaches such as Zubov’s method [6]. However, advances in computational processing have shifted the paradigm towards *polytopic* invariant sets, which are non-conservative but lead to computationally intensive algorithms [7]. Subsequently, the vast majority of recent approaches involve optimization of objective functions that are derived from invariance conditions, over polytopic constraint sets. These invariance conditions are usually algebraic constraints that candidate sets must satisfy for being invariant, and have various characterizations depending on the linearity of the system dynamics, as well as whether they are continuous or discrete in time [7].

Invariant sets for linear systems have been extensively studied. For instance, theoretical considerations for their existence are outlined in [8]. Existing approaches for calculation of invariant polytopes for linear systems include constraint tightening [9], finite-time Aumann integrals [10], MPC schemes [11], state prediction trees [12] and semi-definite programs [13] to name a few. Despite this progress, invariant set computation for linear systems continues to be an active field of research, with recent works focusing on robust invariance [14] and set invariance in the presence of a control action (control invariance) [15]–[19]. Among linear systems, the class of discrete time systems has received considerable attention, following the work in [20]. Approaches include geometric construction using zonotopic bounds [21], Linear Matrix Inequality (LMI)-based algorithms [3], [22], Minkowski partial sums-based approximations [23], [24], linear programming [25], and control invariance using convex optimization [26]. Some of these approaches have also been extended to piecewise affine systems, such as the works in [27]–[30]. Finally, computation of invariant sets for Linear Parameter-Varying (LPV) systems has also been studied, for instance in [31]–[33]. Recently, viability theoretic approaches [34] to modeling disturbances in systems have gained attraction. For example, the authors in [35] model discrete time systems with disturbances as convex difference inclusions and derive invariance conditions. Another example

The authors are with the Department of Electrical Engineering, American University of Sharjah, Sharjah, United Arab Emirates. Emails: {b00066555, smukhopadhyay, nqaddoumi}@aus.edu

is [36], where the authors use differential inclusions to derive control invariant polytopic sets. Similar approaches are used in [37], [38] to model additive state disturbances for computing the minimal RFIS of linear systems.

In contrast, the body of literature on nonlinear systems is relatively limited, where most of the work focuses on discrete-time systems or is restricted to certain classes of nonlinear systems. Examples include [39], where the authors study robust invariance in discrete-time nonlinear systems by lifting the feedback operation to the space of sets, and [40], [41], where the authors compute control invariant sets for such systems using differences of convex functions. For continuous-time nonlinear systems, the focus has primarily been on polynomial dynamics. For example, the authors in [42] use sum of squares relaxations to solve an optimization problem that estimates the region of attraction (ROA) of polynomial systems. Similarly, the authors in [43], [44] formulate this ROA estimation problem as an infinite-dimensional linear program. Yet another approach involves Lyapunov type methods such as the work in [45], and the work in [46], where parameter independent Lyapunov functions are used to characterize invariant sets of polynomial systems with bounded disturbances. Of particular relevance to our work is the work in [47], [48], where a test for invariance is developed based on the sub-tangentiality condition, which compares the angle between the system dynamics and the tangent cone at the boundary of a candidate invariant set [7]. However, due to the computational infeasibility of testing for the condition at infinitely many points, the authors limit the scope of their work to dynamical systems with polynomial vector fields, for which the problem of testing the sub-tangentiality condition is overcome using optimization-based approaches.

All these works use algebraic rather than geometric formulations. This is motivated by the algebraic nature of set invariance conditions, and the concise representation of polytopes as LMIs, which provide convenient formulations for optimization-based approaches. However, no general algebraic framework exists for computing invariant sets for arbitrary nonlinear systems. Subsequently, geometric and computational approaches have attracted some attention. Even so, the majority of computational approaches deal with linear and polynomial systems. Examples can be found in [49]–[51], where polytopic FIS are constructed between ellipsoidal sets, and [52], where geometric methods are used to search for a convex FIS. Other approaches include [53], where the authors determine symmetrical polytopic invariant sets with state, input and rate constraints for systems without disturbances, and [54], where authors derive the maximal robust positively invariant set for linear systems with additive disturbances. Finally, a recent line of computational approaches use data-driven techniques, such as [55], where the authors sample state trajectories starting from a variety of initial conditions to infer invariant sets for discrete time linear systems, and [56], where the authors use machine learning methods for systems whose dynamics are not explicitly modeled with equations.

The most significant advantage of geometric approaches is their ability to generalize to wide classes of systems due to

their non-reliance on the explicit algebraic representation of system dynamics. This is evident from some recent works such as [57]–[59], where closed polytopes are constructed using path planning algorithms on radial graphs for arbitrary nonlinear systems in continuous time, but limited to systems in \mathbb{R}^2 . Another illustration of this can be found in [60], [61], where simplex-based approaches are used for arbitrary nonlinear systems. Besides these limited works, few computation-oriented results are available for generic nonlinear systems [36].

This work focuses on Lipschitz continuous nonlinear systems in continuous time, and computes sequences of polytopic robust forward invariant sets in the presence of bounded additive disturbances. We adopt a geometric approach, using concepts from viability theory [34] and computational topology [62]. Doing so allows us to develop a framework that does not impose any restrictions on the system dynamics, besides the usual conditions for existence and uniqueness of solutions [63]. Further, no additional assumptions on the nature of disturbances are made besides their being bounded and additive. Thus, our approach is valid for a large class of nonlinear systems. To the best of our knowledge, this is the first work that develops an implementable computer algorithm for computing an RFIS of continuous-time nonlinear systems in the presence of disturbances without any further restrictions on state vector dimensions and trajectories. Our strategy is to geometrically deform a polytope into an RFIS using a sequence of homeomorphisms that are guided by an invariance condition. In contrast to previous work, we propose an explicit set of test points and prove that the satisfaction of an invariance condition at these test points is sufficient to conclude that a polytopic set is an RFIS for the system. Thus, the contribution of our work is two-fold:

- We propose a test for invariance of a polytopic RFIS by explicitly identifying test points on the boundary of the polytope.
- We invoke this invariance test to develop an algorithm that is easily implementable, and can generate sequences of invariant sets that vary in size between the maximal and minimal invariant sets. for n -dimensional Lipschitz continuous nonlinear systems with bounded additive disturbances.

The rest of this paper is organized as follows. Section II reviews the necessary mathematical background, and Section III formulates the problem and outlines the approach. In Section IV, an algorithmic test for invariance is developed. It is used as a tool in Section V to develop a computational algorithm for generating sequences of RFISs. Section VI presents the results of implementing this algorithm on a variety of nonlinear systems, and Section VII draws conclusions.

II. MATHEMATICAL BACKGROUND

This section reviews mathematical background used in the rest of the work. Section II-A introduces set-valued maps and Hausdorff distance, which are useful in modeling nonlinear systems with disturbances. Next, it reviews polyhedral sets, simplices and simplicial complexes - which allow modeling of

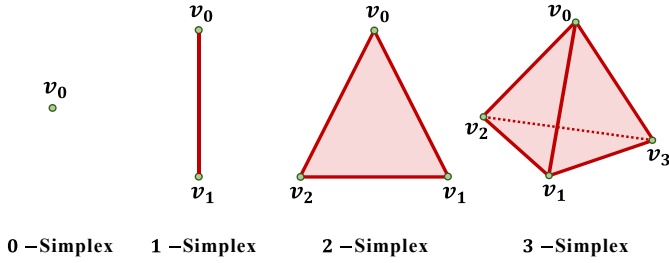


Figure 1. Examples of Simplicies

the boundary of a candidate polytopical RFIS. Finally, it presents vertex maps and their induced homeomorphisms on simplicial complexes, which allow structure-preserving deformations of polytopes. Section II-B formalizes the notion of set invariance.

A. Computational Topology

Definition II.1 (Set-Valued Map). *Let X and Y be topological spaces. $F(\cdot)$ is said to be a set-valued map from X to Y if $F(x) \subset Y \forall x \in X$.*

Set-valued maps are used in defining differential inclusions [64], which are of the form

$$\dot{x}(t) \in F(x(t)), \quad (1)$$

where $F(\cdot)$ is a set-valued map. This work uses differential inclusions to model nonlinear system dynamics in the presence of disturbances, in Section III. Since such sets are fundamental objects for our purposes, it is convenient to review some relevant definitions. We begin with the Hausdorff metric, which is a measure of set-to-set distance.

Definition II.2 (Hausdorff Distance). *The Hausdorff distance between two sets X and Y is denoted $d_H(X, Y)$ and calculated as*

$$d_H(X, Y) = \max \left(\sup_{x \in X} \inf_{y \in Y} \|x - y\|, \sup_{y \in Y} \inf_{x \in X} \|x - y\| \right). \quad (2)$$

Next, we review basics about polyhedra, simplices, simplicial complexes and triangulation using simplices.

Definition II.3 (Polyhedron). *A polyhedron $\mathcal{P} \subset \mathbb{R}^n$ is defined as the intersection of finitely many half-spaces. Thus,*

$$\mathcal{P} = \{x \in \mathbb{R}^n \mid Ax \leq b\}, \quad (3)$$

where $A \in \mathbb{R}^{m \times n}$, $b \in \mathbb{R}^m$ and \leq denotes componentwise inequality.

Bounded polyhedra are called polytopes. A polytope which is also a convex set is said to be a convex polytope. This definition is standard in literature, and convenient for convex optimization based approaches. A convex polytope can be equivalently defined as the convex hull of its vertices [65]:

$$\mathcal{P} = \text{Conv}(\{v_1, \dots, v_m\}), \quad (4)$$

where $\text{Conv}(\cdot)$ represents the convex hull of the set of points $v_1, \dots, v_m \in \mathbb{R}^n$.

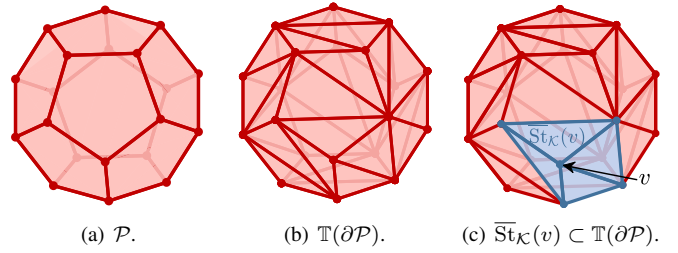


Figure 2. Example of Triangulating the Boundary of a Convex Polytope.

Simplices are generalization of triangles to higher dimensions, and are fundamental objects in algebraic topology, where they are used as building blocks for creating topological manifolds [62].

Definition II.4 (Simplex). *A simplex, $\Delta \subset \mathbb{R}^n$ of dimension k (also called a k -simplex), with $0 \leq k \leq n$ is the convex hull of a set of $(k+1)$ vertex vectors, $\text{Vert}(\Delta) = \{v_0, \dots, v_k\} \subset \mathbb{R}^n$, such that the matrix*

$$B_\Delta = [(v_1 - v_0), \dots, (v_k - v_0)] \in \mathbb{R}^{n \times k} \quad (5)$$

has linearly independent columns.

Since the vertices uniquely define a simplex, we identify Δ with a matrix, $L_\Delta \in \mathbb{R}^{(k+1) \times n}$, where row i of L_Δ is v_{i+1}^T :

$$L_\Delta = [v_0, v_1, \dots, v_k]^T \quad (6)$$

Each face of Δ is defined as the convex hull of a proper subset of $\text{Vert}(\Delta)$. Note that an n -simplex, Δ , itself contains k -simplices where $k < n$. We refer to each of these “sub-simplices” as k -faces of Δ . Figure 1 shows some examples.

We will be interested in $(n-1)$ -simplices embedded in \mathbb{R}^n , and will construct invariant sets with boundaries made up of these simplices. A simplex can have one of two possible orientations, as determined by the ordering of its vertices. For an $(n-1)$ -simplex, $\Delta \subset \mathbb{R}^n$, this orientation is equivalently characterized by the direction of the normal vector to Δ ,

$$(N_\Delta)_i = (-1)^{n+i} \det(B_{\setminus i}), \quad (7)$$

where $(N_\Delta)_i$ is the i -th component of the normal vector, and $B_{\setminus i} \in \mathbb{R}^{(n-1) \times (n-1)}$ is the matrix obtained by deleting the i -th row of B_Δ . Further, an n -simplex, $\Delta \subset \mathbb{R}^n$ has a volume,

$$\text{Vol}(\Delta) = \left| \frac{1}{n!} \det(B_\Delta) \right|. \quad (8)$$

Definition II.5 (Simplicial Complex). *A geometric simplicial complex \mathcal{K} is a set of simplices such that*

- 1) *If $\Delta \in \mathcal{K}$, then for any face Δ' of Δ , we have $\Delta' \in \mathcal{K}$.*
- 2) *If $\Delta_1, \Delta_2 \in \mathcal{K}$, then $\Delta_1 \cap \Delta_2$ is either the empty set or a face of both Δ_1 and Δ_2 .*

A simplicial k -complex is a simplicial complex with the additional property that the largest dimension of any simplex in \mathcal{K} equals k . Finally, a *homogeneous simplicial k -complex* is a simplicial complex where every simplex of dimension less than k is a face of a k -simplex [62]. In the remainder

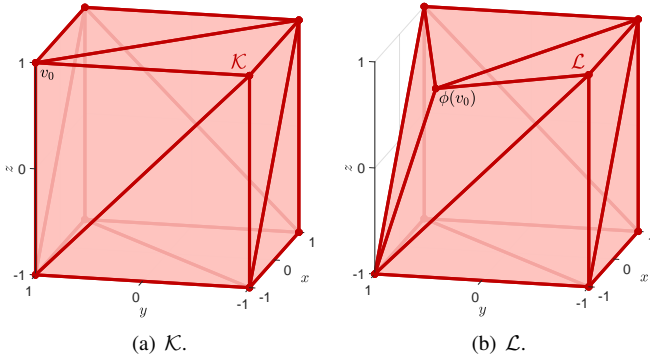


Figure 3. Example of an induced homeomorphism from \mathcal{K} to \mathcal{L} .

of this work, we will take a simplicial complex to mean a homogeneous simplicial $(n - 1)$ -complex in \mathbb{R}^n . These simplicial complexes are particularly relevant to our work because they triangulate convex polytopes, which will serve as a starting point for our algorithm. The triangulation of the boundary of a polytope \mathcal{P} , denoted $\mathbb{T}(\partial\mathcal{P})$, is a set of simplices that partition $\partial\mathcal{P}$, such that their union is the boundary of the polytope and the intersection of the interiors of any two simplices in $\mathbb{T}(\partial\mathcal{P})$ is empty. This is illustrated for a dodecahedron in Fig. 2. Figure 2(a) shows the polytope \mathcal{P} , whereas Fig. 2(b) shows the polytope with triangulated boundary. Each triangle on the boundary is a simplex, and the set of all simplices that form the boundary is a simplicial complex, $\mathcal{K} = \mathbb{T}(\partial\mathcal{P})$. The set of all 0-faces of \mathcal{K} is then given by $\text{Vert}(\mathcal{K}) = \bigcup_{\Delta \in \mathcal{K}} \text{Vert}(\Delta)$. Given a vertex $v \in \text{Vert}(\mathcal{K})$, we denote the closed star of v as $\overline{\text{St}}_{\mathcal{K}}(v)$, which is the set of all simplices in \mathcal{K} that contain v as a 0-face. For a homogeneous simplicial $(n - 1)$ -complex embedded in \mathbb{R}^n , this is easily visualized, as shown in Fig. 2(c). Observe that $\overline{\text{St}}_{\mathcal{K}}(v)$ is itself a simplicial complex.

We also remark that a convex polytope \mathcal{P} , being a convex compact subset of \mathbb{R}^n forms a topological n -manifold with boundary [66]. Therefore, $\partial\mathcal{P}$ forms an $(n - 1)$ -manifold [67]. Following standard notation, we denote the geometric realization of \mathcal{K} by $|\mathcal{K}|$, which is the topological space obtained by gluing all the simplices together, as determined by their faces. Since $\mathbb{T}(\partial\mathcal{P})$ and \mathcal{K} are the same set, it follows that $\partial\mathcal{P}$ and $|\mathcal{K}|$ are homeomorphic topological manifolds [62]. Recall that two topological manifolds X and Y are homeomorphic if $\exists g : X \rightarrow Y$ such that g is invertible, and both g and g^{-1} are continuous.

In order to deform polytopes, it is convenient to study homeomorphisms between them. Homeomorphisms will be used in our work to deform polytopes into robust forward invariant sets. These homeomorphisms are induced from simplicial maps with the help of barycentric coordinates as explained in what follows. Simplicial maps are mappings between simplicial complexes that are the natural equivalent of continuous maps between topological spaces. A *vertex map* between two simplicial complexes \mathcal{K} and \mathcal{L} is a function $\phi : \text{Vert}(\mathcal{K}) \rightarrow \text{Vert}(\mathcal{L})$ such that the vertices of every simplex in \mathcal{K} map to the vertices of a simplex in \mathcal{L} . ϕ can

be extended to a continuous map $g : |\mathcal{K}| \rightarrow |\mathcal{L}|$, as

$$g(x) = \sum_{i=0}^N b_i(x) \phi(v_i), \quad (9)$$

where $b_i(x)$ are the barycentric coordinates of x , defined in the next paragraph. The continuous map g is called the “induced map” due to ϕ , and is unique for a given vertex map. Further, if ϕ is bijective, and $\phi^{-1} : \text{Vert}(\mathcal{L}) \rightarrow \text{Vert}(\mathcal{K})$ is also a vertex map, then g is a homeomorphism between $|\mathcal{K}|$ and $|\mathcal{L}|$ [62]. An example is illustrated in Fig. 3, where \mathcal{K} triangulates a cube with vertices $(\pm 1, \pm 1, \pm 1)$ as shown in Fig. 3(a). The vertex map $\phi : \text{Vert}(\mathcal{K}) \rightarrow \text{Vert}(\mathcal{L})$ maps $v_0 = (-1, 1, 1)$ to $\phi(v_0) = (-0.7, 0.5, 0.7)$ and all other vertices to themselves. The resulting simplicial complex, \mathcal{L} is shown in Fig. 3(b).

The barycentric coordinates of a point x may be found as follows. Let \mathcal{K} be a simplicial complex with $\text{Vert}(\mathcal{K}) = \{v_0, v_1, \dots, v_N\}$. Let the set of indices $\mathcal{A} = \{\alpha_0, \alpha_1, \dots, \alpha_{n-1}\} \subset \{0, 1, \dots, N\}$, so that a given simplex, $\Delta \in \mathcal{K}$ has $\text{Vert}(\Delta) = \{v_{\alpha_0}, \dots, v_{\alpha_{n-1}}\}$. Thus, any point $x \in \Delta$ can be written as $x = \sum_{i \in \mathcal{A}} \lambda_i v_i$, with $\sum_{i \in \mathcal{A}} \lambda_i = 1$ and $\lambda_i \geq 0 \forall i$. The *barycentric coordinates* of a point $x \in \Delta$ are obtained by setting $b_i(x) = \lambda_i \forall i \in \mathcal{A}$ and $b_i(x) = 0 \forall i \notin \mathcal{A}$. Note that a point in a homogeneous simplicial $(n - 1)$ -complex can be identified by its barycentric coordinates, as $b_i(x)$ is unique even if the point lies in the intersection of multiple simplices of the complex.

Another concept from computational topology that we will use is simplex subdivision. A simplex subdivision of Δ , denoted $\mathbb{S}(\Delta)$ is a simplicial complex obtained by introducing new vertices in the interior of the simplex, $\text{int}(\Delta)$, and constructing a triangulation of Δ . We overload notation and use $\mathbb{S}(\mathcal{K})$ to represent the simplicial complex obtained as

$$\mathbb{S}(\mathcal{K}) = \bigcup_{\Delta \in \mathcal{K}} \mathbb{S}(\Delta). \quad (10)$$

There are two key properties: First, the vertices of the simplices in $\mathbb{S}(\Delta)$ can be ordered so that the normal direction for each $s \in \mathbb{S}(\Delta)$ is the same as that of Δ . Second, the geometric realization of the subdivision is the same as that of the original complex, i.e. $|\mathbb{S}(\mathcal{K})| = |\mathcal{K}|$ [62]. Thus, subdivision does not change the normal directions or the geometric realization.

There are several ways to introduce new vertices in the interior of the simplex for subdivision. Examples include centroidal and barycentric subdivisions, which are illustrated in Fig. 4. We will denote the resulting simplicial complexes with $\mathbb{S}_C(\cdot)$ and $\mathbb{S}_B(\cdot)$ respectively. Given a k -simplex, Δ , we can construct $\mathbb{S}_C(\Delta)$ and $\mathbb{S}_B(\Delta)$ knowing only $\text{Vert}(\Delta)$. In particular, $\mathbb{S}_C(\Delta)$ subdivides a k -simplex into three k -simplices by introducing a new vertex at the centroid of Δ , (the coordinate of which can easily be calculated as $v_b = \frac{1}{k+1} \sum_{i=0}^k v_i$), and connecting each v_b to $v_i \forall i$. Similarly, $\mathbb{S}_B(\Delta)$ introduces new coordinates at the barycentre of all faces of Δ . The vertices of Δ are connected to the new vertices iteratively (see [62] for procedure).

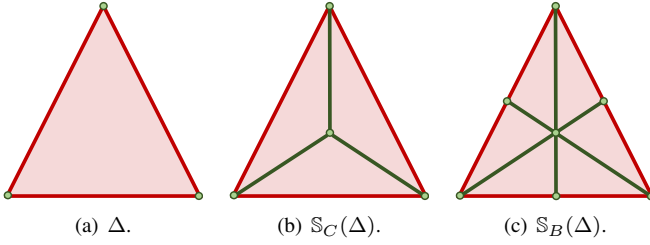


Figure 4. Subdividing a Simplex.

B. Robust Forward Set Invariance

The performance and robustness of a dynamical system can be characterized by forward invariance. A subset of the system's state space is said to be a forward invariant set (FIS) if no system trajectory that begins in the set leaves it at any future time. Further, the set is said to be a Robust FIS (RFIS) if it is an FIS in the presence of disturbances.

Definition II.6 (Robust Forward Invariant Set). *Let $S \subset \mathbb{R}^n$ represent the state space of a given dynamical system, $\dot{x}(t) = f(x(t), \omega(t))$, where $\omega(t) : [0, \infty) \rightarrow \Omega$ is a bounded disturbance function that takes values in Ω . Further, let \mathcal{X} represent the set of solutions for this system. A set $\mathcal{R} \subset S$ is said to be an RFIS if $\forall x \in \mathcal{X}, x(t_0) \in \mathcal{R} \implies x(t) \in \mathcal{R} \forall t \geq t_0$.*

The *minimal* RFIS is a set \mathcal{R}_s such that no proper subset of \mathcal{R}_s is an RFIS for the system. Conversely, the maximal RFIS, \mathcal{R}_m is not a proper subset of any RFIS.

III. PROBLEM FORMULATION

Consider a non-linear system with bounded additive disturbances modeled by a differential inclusion $\dot{x}(t) \in F(x(t))$, where $F(\cdot)$ is a set-valued map. Specifically,

$$\dot{x}(t) \in F(x(t)) \quad (11a)$$

$$F(x(t)) = \{f(x(t)) + \omega(t) \mid \omega(t) \in \Omega \forall t \in [0, \infty)\}. \quad (11b)$$

Here, $f : S \rightarrow \mathbb{R}^n$ models the dynamical system with state space $S \subset \mathbb{R}^n$, and $\omega : [0, \infty) \rightarrow \Omega$ is the disturbance function, where $\Omega \subset \mathbb{R}^n$ is the bounded noise space. If $\Omega = \{0\}$, the dynamics reduce to the usual $\dot{x}(t) = f(x(t))$. The standard conditions for existence and uniqueness of solutions [63] are assumed to be met. Thus, $F(\cdot)$ is assumed to be Lipschitz continuous in the Hausdorff metric, so that

$$d_H(F(x), F(y)) \leq \ell \|x - y\| \quad \forall x, y \in \mathcal{X}, \quad (12)$$

where ℓ is the Lipschitz constant for the system. Starting with a polytope $\mathcal{P} \subset \mathcal{X}$ and a simplicial complex \mathcal{K} that triangulates $\partial\mathcal{P}$, the objective is to find families of polytopical RFISs for the system in (11).

The proposed strategy begins with a simplicial complex \mathcal{K} such that $|\mathcal{K}| = \partial\mathcal{P}$, where \mathcal{P} is a convex polytope. Since \mathcal{P} is a topological manifold that can be identified uniquely by its boundary, we apply a sequence of homeomorphisms on $|\mathcal{K}|$ to geometrically deform \mathcal{P} so that it sequentially approximates either \mathcal{R}_s or \mathcal{R}_m . These deformations are vertex maps on

0-faces in \mathcal{K} and its subdivisions, such that all simplices satisfy a **Boundary Condition**. We first develop this condition and show that if all simplices in \mathcal{K} satisfy the **Boundary Condition**, then $|\mathcal{K}|$ is the boundary of an RFIS. This serves as a computational invariance test that decides whether a deformation is to be kept or discarded. The proposed algorithm can be easily implemented knowing only the system dynamics and the coordinates of the 0-faces in \mathcal{K} .

IV. INVARIANCE TEST

Let \mathcal{K} be a simplicial complex that triangulates the boundary of a polytope $\mathcal{P} \subset \mathbb{R}^n$, and Δ be a simplex in \mathcal{K} . An example is the dodecahedron in Fig. 2. Let $x \in \Delta$ be any point on the simplex. Note that $|\mathcal{K}| = \partial\mathcal{P}$, and $x \in \Delta \implies x \in \partial\mathcal{P}$. In this section, we develop a computational tool to decide whether \mathcal{K} triangulates the boundary of an RFIS, for a system with dynamics given in (11).

Let set $A \subset \mathbb{R}^n$ and vector $b \in \mathbb{R}^n$. Let $\langle A, b \rangle$ denote $\sup_{a \in A} \langle a, b \rangle$, where $\langle \cdot, \cdot \rangle$ is the standard inner product.

Definition IV.1 (Invariance Condition). *A point $x \in \Delta \in \mathcal{K}$ is said to satisfy the **Invariance Condition** if*

$$\langle F(x), N_\Delta \rangle \leq 0, \quad (13)$$

where N_Δ is the outward unit normal vector to Δ .

Note that the **Invariance Condition** is related to the subtangentiality condition [7]. It is a condition on the angle between the extreme ray of the tangent cone to the dynamics F given in (11), and the normal vector to the simplex Δ , at x . This is illustrated in Fig. 5 where two boundary points are shown. Here, $x(t_0)$ does not satisfy the **Invariance Condition**, but $x(t_1)$ does. If a system trajectory finds itself at $x(t_0)$, then it may escape the set through the boundary point $x(t_0)$, i.e. for some disturbance ω , $\exists \varepsilon$ such that $x(t_0 - \varepsilon) \in \mathcal{P}$ but $x(t_0 + \varepsilon) \notin \mathcal{P}$. However, no disturbance $\omega \in \Omega$ can result in a system trajectory escaping the set through $x(t_1)$. Similar boundary conditions have been used in works such as [48], [58]–[61] for arbitrary sets, but the novelty of this work is in the development of an implementable invariance test and its invocation to perform geometric deformations. The above intuition that the **Invariance Condition** being satisfied at each point on the set implies that system trajectories cannot escape the set is proved in the result below.

Theorem IV.2. *If $x_0 \in \Delta \in \mathcal{K}$ satisfies the **Invariance Condition**, then no system trajectory can escape the set \mathcal{P} through x_0 .*

Proof. We prove the contrapositive of this statement, i.e. If a system trajectory escapes the set \mathcal{P} through $x(t_0) \in \Delta$, then $\langle F(x(t_0)), N_\Delta \rangle > 0$. Let $\omega(t) : [0, \infty) \rightarrow \Omega$ be the disturbance function that resulted in this trajectory, so that $\dot{x}(t) = f(x(t)) + \omega(t)$, and let $x(t_0) \in \partial\mathcal{P}$. Since the system trajectory escapes \mathcal{P} through $x(t_0)$, $\exists \delta > 0$ such that $x(t_0 + \delta) \notin \mathcal{P}$. However,

$$\begin{aligned} x(t_0 + \delta) &= x(t_0) + \delta \times \dot{x}(t_0) + O(\delta^2) \\ &= x(t_0) + \delta \times (f(x(t_0)) + \omega(t_0)) + O(\delta^2). \end{aligned} \quad (14)$$

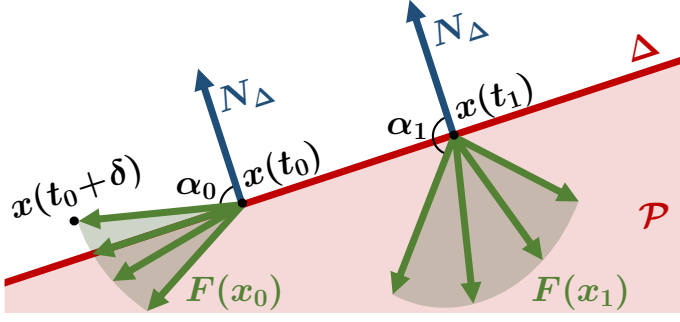


Figure 5. Angle between normal vector and extreme ray of system dynamics

As $\delta \rightarrow 0$,

$$x(t_0 + \delta) - x(t_0) \rightarrow \delta \times (f(x(t_0)) + \omega(t_0)). \quad (16)$$

Let $y(\delta) = x(t_0 + \delta) - x(t_0)$ for convenience, Since N_Δ is normal to the simplex by definition, it follows that the angle between N_Δ and $y(\delta) < \frac{\pi}{2}$, whenever $\delta > 0$. This is because $y(\delta)$ is simply the vector from the point on $\partial\mathcal{P}$ to the point on the trajectory at time $t_0 + \delta$, which lies *outside* \mathcal{P} . It then follows from (16) that

$$\alpha_0 = \cos^{-1} \left(\frac{\langle \delta \times (f(x(t_0)) + \omega(t_0)), N_\Delta \rangle}{\|\delta \times (f(x(t_0)) + \omega(t_0))\| \times \|N_\Delta\|} \right) < \frac{\pi}{2}. \quad (17)$$

Cancelling δ , and taking the cosine of both sides due to it being monotone decreasing over $[0, \frac{\pi}{2})$, it follows that

$$\langle f(x(t_0)) + \omega(t_0), N_\Delta \rangle > 0 \quad (18)$$

$$\implies \sup_{\nu(t_0) \in \Omega} \langle f(x(t_0)) + \nu(t_0), N_\Delta \rangle > 0 \quad (19)$$

$$\implies \langle F(x(t_0)), N_\Delta \rangle > 0, \quad (20)$$

which proves the desired statement. \square

Corollary IV.2.1. *If every point $x \in \Delta$ satisfies the **Invariance Condition**, then no system trajectory can escape \mathcal{P} through $\Delta \in \mathbb{T}(\partial\mathcal{P})$. We call such a Δ as an “invariant simplex”.*

Corollary IV.2.2. *If every $\Delta \in \mathcal{K}$ is an invariant simplex, then \mathcal{P} is an RFIS.*

Proof. $x \in \partial\mathcal{P} \implies x \in \bigcup_{\Delta \in \mathcal{K}} \Delta$. But, no system trajectory can escape \mathcal{P} through any such Δ (by Corollary IV.2.1). Thus, all system trajectories stay in \mathcal{P} , making it an RFIS. \square

Note that if $x \in \Delta_1 \cap \Delta_2$, it must satisfy the **Invariance Condition** with respect to both simplices. Hence, Theorem IV.2 is a test for invariance, as the inner product between the normal vector and the system dynamics can be easily computed. The only caveat is that for a given polytope \mathcal{P} to be invariant, every point on $\partial\mathcal{P}$ must satisfy the **Invariance Condition**, and it is computationally impossible to test infinitely many points. However, when $F(\cdot)$ is Lipschitz continuous, this constraint can be overcome as follows.

Theorem IV.3. *Let F be ℓ -Lipschitz with respect to the Hausdorff metric. Let $x_0 \in \Delta$, where Δ is a simplex with*

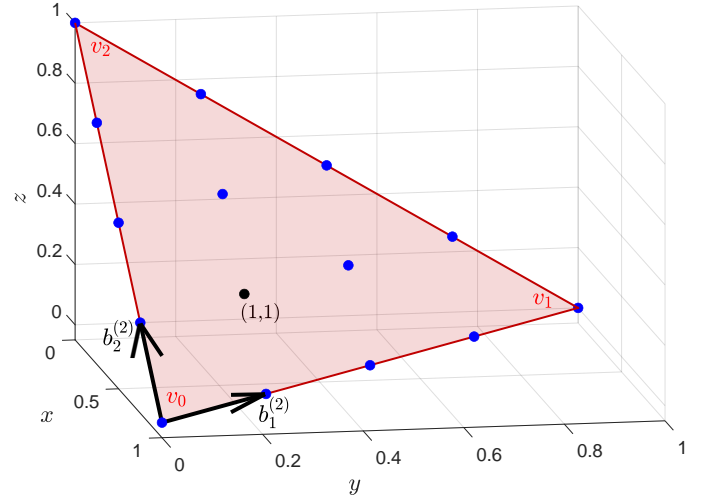


Figure 6. Standard Simplex with Coordinate System

normal vector, N_Δ . If $\exists \varepsilon > 0$ such that $\langle F(x_0), N_\Delta \rangle \leq -\varepsilon$, then $\langle F(x), N_\Delta \rangle \leq 0 \forall x$ such that $\|x - x_0\| \leq \frac{\varepsilon}{\ell}$.

Proof. This follows from Proposition 3 in [60]. \square

Based on Theorems IV.2 and IV.3, we develop an algorithm to check if Δ is invariant by testing for a variant of the **Invariance Condition** at finitely many points. We call this variant the **Boundary Condition**, which requires the inner product to not just be negative but sufficiently negative to ensure that points in an appropriate neighborhood of these test points satisfy the **Invariance Condition**.

A. Test Point Generation

We present an implementable method to generate a finite set of test points, $\mathcal{T}_m \subset \Delta$, and show how a simple calculation at these points can decide whether Δ is an invariant simplex. To the best of our knowledge, no explicit set of test points has been proposed in previous work - we prove that testing for a variant of the **Invariance Condition** at these test points can circumvent the problem of testing at infinitely many points. The set, \mathcal{T}_m is a lattice, generated a priori on a reference simplex and then mapped to Δ using a linear transformation. Although lattices on simplices are used in other applications like the study of mixtures [68], the method proposed here generates the lattice using only $\text{Vert}(\Delta)$.

1) *Generating Lattice on Reference Simplex:* Let Λ be the standard simplex in \mathbb{R}^n , defined as

$$\Lambda = \left\{ \lambda \in \mathbb{R}^n \mid \sum_{i=1}^n \lambda_i = 1, \lambda_i \geq 0 \right\}. \quad (21)$$

To control the coarseness of the lattice, a parameter $\delta_m \in (0, 1]$ is introduced. Here, m is the iteration number in the algorithm to test for invariance. Since we would like the lattice to get exponentially finer, we set

$$\delta_m = 2^{-m}, \quad m = 0, 1, \dots, m_{\max}, \quad (22)$$

where m_{\max} is the maximum allowed iteration number for the algorithm. In order to identify test points on the simplex, we introduce a new coordinate system for each value of m and introduce a condition that guarantees that a given point in this coordinate system lies on the simplex. The change of basis allows us to easily identify the test points.

Lemma IV.4. For a fixed m such that $0 \leq m \leq m_{\max}$, consider a coordinate system with v_0 as the origin, and $(n-1)$ basis vectors given by

$$b_j^{(m)} = v_0 + \delta_m (v_j - v_0), \quad j = 1, \dots, n-1. \quad (23)$$

In this coordinate system, a point $a = (a_1, \dots, a_{n-1})$ is in Λ if and only if $\sum_{i=1}^{n-1} a_i \in [0, \delta_m^{-1}]$.

Proof. Writing out (a_1, \dots, a_{n-1}) using the basis vectors gives

$$\sum_{i=1}^{n-1} a_i b_i^{(m)} = \sum_{i=1}^{n-1} a_i (v_0 + \delta_m (v_i - v_0)) \quad (24)$$

$$= \left(\sum_{i=1}^{n-1} \delta_m a_i v_i \right) + (1 - \delta_m) v_0 \sum_{i=1}^{n-1} a_i \quad (25)$$

Let $a_0 = \frac{1 - \delta_m \sum_{i=1}^{n-1} a_i}{\delta_m}$, so that the point a can be written as $\sum_{i=0}^{n-1} \delta_m a_i v_i$ with respect to the standard basis. Further, $\sum_{i=0}^{n-1} \delta_m a_i = 1$ and $0 \leq \delta_m a_i \leq 1 \forall i$, whenever $a_i \in [0, \delta_m^{-1}]$. Hence, the point is written as a convex combination of the vertices of the simplex, and therefore lies in it. \square

Next, we define a lattice of test points on the standard simplex as follows. This lattice will later be mapped to the test simplex through a linear transformation.

Definition IV.5 (Lattice Test Point). $a = (a_1, \dots, a_{n-1})$ is a lattice test point if $a \in \Delta$ and $a_i \in \mathbb{N}_0 = \{0, 1, 2, \dots\} \forall 1 \leq i \leq n-1$.

For instance, the 2-simplex Λ in \mathbb{R}^3 with vertices v_0, v_1 and v_2 is shown in Fig. 6 for $m = 2$, along with the basis vectors $b_1^{(2)}$ and $b_2^{(2)}$, and the test point $(a_1, a_2) = (1, 1)$. Note that the vertices of Λ are always included in the lattice for all m .

Thus, all lattice points can be computed a priori in this coordinate system and then represented in the standard coordinate system for all values of $0 \leq m \leq m_{\max}$. It follows from the construction that the number of test points generated in iteration m for an $(n-1)$ -simplex in \mathbb{R}^n with parameter δ_m is

$$l_m = \binom{\delta_m^{-1} + n - 1}{\delta_m^{-1}} = \frac{(\delta_m^{-1} + n - 1)!}{\delta_m^{-1}! \times (n - 1)!}. \quad (26)$$

2) *Mapping test points to a simplex in the simplicial complex that triangulates the boundary of a polytope:* The l_m coordinates generated on the standard simplex as described above are stored as rows of a matrix, $M_m \in \mathbb{R}^{l_m \times n}$. Note that this representation is in the standard basis. We use the m subscript to emphasize the dependence on δ_m , and note that M_m can be computed a priori for different m . To obtain the

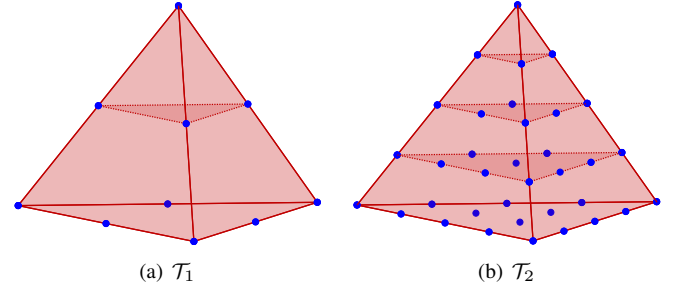


Figure 7. Lattice of Test Points for a 3-Simplex

lattice points on the simplex of interest, Δ , we perform the following linear transformation, $T: M_m \rightarrow \mathbb{R}^{l_m \times n}$ given as

$$T(M_m) = M_m L_\Delta. \quad (27)$$

Let

$$\mathcal{T}_m = \{x \in \mathbb{R}^n \mid x \text{ is a row of } T(M_m)\}, \quad (28)$$

be the set of all proposed test points on Δ . For instance, Fig. 7 shows \mathcal{T}_1 and \mathcal{T}_2 for a 3-simplex. Note that a set of 3-simplices would triangulate the boundary of a 4-dimensional RFIS.

We now prove that the generated test lattice is indeed on the simplex, and that it is sufficient to check for a variant of the **Boundary Condition** at only these lattice points to guarantee that the simplex is invariant.

Lemma IV.6. $\mathcal{T}_m \subset \Delta$.

Proof. See Appendix A. \square

Thus, all test points calculated on Λ map to the desired simplex, Δ under the transformation $T(\cdot)$. These test points can be used to determine whether or not a given simplex is invariant, using the following theorem.

Theorem IV.7. Let Δ be a given simplex with $\text{Vert}(\Delta) = \{v_0, \dots, v_{n-1}\}$, $r = \max_{i,j} \|v_i - v_j\|$, and \mathcal{T}_m be the set of test points on Δ for a given δ_m . Suppose that

$$\langle F(x), N_\Delta \rangle \leq -r \delta_m \ell, \quad \forall x \in \mathcal{T}_m \quad (29)$$

where ℓ is the Lipschitz constant for the system dynamics given by F . Then, Δ is an invariant simplex.

Proof. See Appendix B. \square

A test point that satisfies (29) is said to satisfy the **Boundary Condition**. Theorem IV.7 is a tool to test whether Δ is an invariant simplex. This process of testing whether a given simplex is invariant is summarized in Algorithm 1. The algorithm is named BCD_Test since it generates the set of test points on the simplex and checks whether they satisfy the **Boundary Condition**. It takes as input the simplex, which it identifies by its vertices. Additionally, the system dynamics F , Lipschitz constant ℓ , and the maximum number of iterations to run the algorithm m_{\max} are also input to the algorithm. Further, the algorithm also has access to the constants δ_m , M_m , l_m which are computed a priori and stored in memory. The algorithm computes the ratio of test points for which the

Boundary Condition is not satisfied to the total number of test points when $\delta_m = 2^{-m_{\max}}$, denoted \mathcal{N} . Note that Δ is invariant if $\mathcal{N} = 0$.

Line 1 of Algorithm 1 computes the matrix L_Δ , and line 2 computes $r = \max_{i,j} \|v_i - v_j\|$, which is the length of the longest 1-face of the simplex. Line 3 computes the normal vector to the simplex using (7). The invariance condition is then checked on the test points that successively get finer in each iteration m . Observe from (29) that as m increases - so do the number of points that must satisfy the **Boundary Condition**, but the condition on how negative the inner product $\langle F(x), N_\Delta \rangle$ must be is progressively relaxed. Thus, iteration m of the **for** loop in line 4 begins by initializing $\mathcal{N}_m = 0$, where \mathcal{N}_m counts the number of test points that violate the **Boundary Condition**. Note that checking the **Boundary Condition** at finitely many points is equivalent to matrix-vector multiplication. Since each row of the matrix $T(M_m)$ computed in line 6 is a test point, we denote by $F(T(M_m))$ the matrix whose corresponding row is the result of evaluating $F(\cdot)$ at these test points. Since the normal vector is the same for all these test points, the inner product can be computed as in line 7. The result is a vector \mathcal{IP} containing the values of the inner product at each test point. If all entries are sufficiently negative for any m as determined by Theorem IV.7, then we are guaranteed that the simplex is invariant. Thus, the **foreach** loop in line 8 counts the number of test points that violate the **Boundary Condition**. If this number is 0 for any m , then the algorithm returns $\mathcal{N} = 0$ and declares the simplex to be invariant. If not, then it increments m until the maximum allowed iteration m_{\max} is reached, and outputs $\mathcal{N}(\Delta)$ as the ratio of test points that violate the **Boundary Condition** to the total number of test points l_m when $m = m_{\max}$, as computed in line 18. Here, $0 \leq \mathcal{N}(\Delta) \leq 1$ is a measure of how close Δ is to being invariant.

The next section invokes this simplex invariance test to perform geometric deformations that attempt to transform convex polytopes to robust forward invariant sets.

V. RFIS COMPUTATION ALGORITHM

In this section, we use Algorithm 1 as a tool in developing a polytopical RFIS computation algorithm.

A. Proposed Vertex Map

We are interested in systems with a non-trivial minimal RFIS, \mathcal{R}_s and maximal RFIS, \mathcal{R}_m . Thus, \mathcal{R}_s is not just a point, and \mathcal{R}_m does not enclose infinite volume. We begin with a convex polytope \mathcal{P} , such that $\mathcal{R}_s \subset \mathcal{P}$, and triangulate \mathcal{P} by a simplicial complex \mathcal{K} , such that $\text{Vert}(\mathcal{K}) = \{v_0, \dots, v_N\}$.

Consider a point $c \in \text{int}(\mathcal{R}_s)$. Note that although \mathcal{R}_s is not known, c may easily be chosen. If the RFIS is due to a known equilibrium point, then c can be chosen as this point. Else, if it is due to a known limit cycle, c can be chosen as any point in the interior of the cycle. We consider deformations where

Algorithm 1: BCD_Test (Boundary Condition Test)

Inputs : $\text{Vert}(\Delta), F, \ell, m_{\max}$
Constants: $\delta_m, M_m, l_m \forall 1 \leq m \leq m_{\max}$
Outputs : $\mathcal{N}(\Delta)$

- 1 Compute L_Δ from $\text{Vert}(\Delta)$ using (6)
- 2 Compute $r = \max \|v_i - v_j\|$, where $v_i, v_j \in \text{Vert}(\Delta)$
- 3 Compute N_Δ using (7) // Normal vector
- 4 **for** $m \in \{0, 1, \dots, m_{\max}\}$ **do**
- 5 Set $\mathcal{N}_m = 0$
- 6 Compute $T(M_m)$ using (27)
- 7 Compute $\mathcal{IP} = F(T(M_m))N_\Delta$ // Vector of
//inner products at all test points
- 8 **foreach** component x of \mathcal{IP} **do**
- 9 **if** $x > -r\delta_m\ell$ **then**
- 10 $\mathcal{N}_m = \mathcal{N}_m + 1$
- 11 **end**
- 12 **end**
- 13 **if** $\mathcal{N}_m == 0$ **then**
- 14 **return** $\mathcal{N}(\Delta) = 0$
- 15 **end program**
- 16 **end**
- 17 **end**
- 18 **return** $\mathcal{N}(\Delta) = \frac{\mathcal{N}_m}{l_m}$ // $0 \leq \mathcal{N}(\Delta) \leq 1$

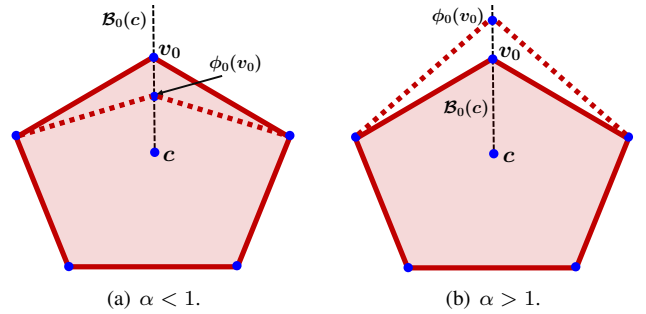


Figure 8. Vertex map ϕ_0 when $\alpha < 1$ and $\alpha > 1$.

all vertices but one are mapped to themselves. Specifically, $\phi_j : \text{Vert}(\mathcal{K}) \rightarrow \text{Vert}(\mathcal{L})$ is defined as

$$\phi_j(v_i) = \begin{cases} v_i, & i \neq j \\ (1 - \alpha)c + \alpha v_i, & i = j \end{cases}, \quad (30)$$

where $\alpha > 0$ is a growth/decay parameter. Hence, the vertex map ϕ_i only perturbs the vertex v_i by moving it along a ray $\mathcal{B}_i(c)$ emanating from c and containing v_i :

$$\mathcal{B}_i(c) = \{c + \lambda(v_i - c) \mid \lambda > 0\}. \quad (31)$$

An illustration is provided for the case where a simplicial complex of 1-simplices triangulates the boundary of a 2-dimensional polytope (a pentagon) in Fig. 8. The vertex v_0 is mapped to $\phi_0(v_0)$ which is constrained on the ray $\mathcal{B}_0(c)$.

Observe that only the points in the closed star of the perturbed vertex are changed due to the vertex map. It follows that $g_j(x) = x$ if $x \notin \text{St}_{\mathcal{K}}(v_j)$, where $g_j : |\mathcal{K}| \rightarrow |\mathcal{L}|$ is the induced map due to ϕ_j , as defined in (9). We now show that the deformed polytope is homeomorphic to the initial polytope.

Theorem V.1. *Let g_j be the induced map due to ϕ_j as defined in (30). If $\alpha > 0$, then g_j is a homeomorphism $\forall j$.*

Proof. A vertex map induces a homeomorphism if and only if it has an inverse that is also a vertex map. Clearly, the map defined by

$$\phi_j^{-1}(v_i) = \begin{cases} v_i, & i \neq j \\ (1 - \alpha^{-1})c + \alpha^{-1}v_i, & i = j \end{cases}, \quad (32)$$

is the inverse map if $\phi_j(v_i) \neq \phi_j(v_k) \forall j$ and $\forall i \neq k$. Since $\alpha > 0$, it follows that $\phi_j(v_i) \in \mathcal{B}_i(c)$. Since $c \in \text{int}(\mathcal{P})$, and since the simplicial complex triangulates the boundary of the convex polytope \mathcal{P} , no two of its vertices lie on the same ray. Thus, $\mathcal{B}_i(c) \cap \mathcal{B}_k(c)$ is the empty set, and no two vertices are ever mapped to the same point, making ϕ_j a bijective vertex map. Hence, its induced map, g_j is a homeomorphism. \square

Corollary V.1.1. *Let $\phi : \text{Vert}(\mathcal{K}) \rightarrow \text{Vert}(\mathcal{L})$ be defined as*

$$\phi(v_i) = \phi_{j_k} \circ \dots \circ \phi_{j_1}(v_i), \quad (33)$$

where ϕ_{j_i} are vertex maps as defined in (30). Then, the geometric realization $|\mathcal{L}|$ is homeomorphic to the geometric realization $|\mathcal{K}|$.

Proof. First, note that the vertex map $\phi(v_i)$ in (33) entails the application of ϕ_{j_1} followed by ϕ_{j_2} . If $v_i \in \mathcal{B}_i(c)$, then $\phi_{j_1}(v_i) \in \mathcal{B}_i(c)$ by definition. Since $\mathcal{B}_i(c) \cap \mathcal{B}_k(c)$ is the empty set, ϕ_{j_2} is also a bijective vertex map and induces a homeomorphism. Since the composition of two homeomorphisms is also a homeomorphism, and since any finite sequence of the vertex maps in (30) restricts the image of v_i to $\mathcal{B}_i(c)$, it follows by induction that $\phi_{j_k} \circ \dots \circ \phi_{j_1}$ also induces a homeomorphism. Thus, $|\mathcal{K}|$ and $|\mathcal{L}|$ are homeomorphic. \square

The vertex map in (33) deforms the polytope into a manifold that is homeomorphic to it. Therefore, the deformations preserve the topological structure of the polytope, so that the simplicial complex obtained by the sequence of deformations triangulates the boundary of a new polytope. This new polytope need not be convex, since homeomorphisms do not preserve convexity in general. However, it is not self-intersecting since $\phi(v_i) \in \mathcal{B}_i(c) \forall i$. A vertex map is either kept or discarded depending on whether or not it serves the objective of approximating an RFIS. For this, we require a measure of how ‘‘close’’ a given simplex Δ is to being invariant. One such measure is $\mathcal{N}(\Delta)$, the ratio of test points on Δ that violate the **Boundary Condition**, to the total number of test points on Δ . We propose that a vertex perturbation $\phi : \text{Vert}(\mathcal{K}) \rightarrow \text{Vert}(\mathcal{L})$ be kept if

$$\left(\sum_{\Delta \in \mathcal{L}} \mathcal{N}(\Delta) < \sum_{\Delta \in \mathcal{K}} \mathcal{N}(\Delta) \right) \text{ or } \sum_{\Delta \in \mathcal{L}} \mathcal{N}(\Delta) = 0, \quad (34)$$

and discarded otherwise.

B. Polytopic RFIS Computation Algorithm

This section presents an algorithm to compute RFISs of different sizes for a given non-linear ℓ -Lipschitz dynamical system with bounded additive disturbances. The essence of the algorithm is to repeatedly perturb vertices in the simplicial triangulation through vertex maps so that each test point in all the simplices satisfies the **Boundary Condition**. A particularly interesting application of this is when \mathcal{P} itself is an RFIS for the system obtained through any other method. Each deformation would result in a smaller or larger RFIS depending on whether $\alpha < 1$ or $\alpha > 1$, thereby creating an RFIS family. The appropriate RFIS may be considered for the application in concern. Once a stage is reached where no vertex can be perturbed further (all perturbations would violate (34)), the simplices in the simplicial complex \mathcal{L} are subdivided. Since the geometric realizations before and after the subdivision are the same, i.e. $|\mathbb{S}(\mathcal{L})| = |\mathcal{L}|$, it follows that the application of vertex maps of the form in (33) preserves homeomorphicity. On the other hand, since $\overline{\text{St}}_{\mathbb{S}(\mathcal{K})}(v) \subset \overline{\text{St}}_{\mathcal{K}}(v)$, the deformations are finer, allowing the new polytope to better approximate the shape of the RFIS. This allows for a family of algorithms, each with different types and sequences of simplicial deformations and subdivisions. One such algorithm is presented in Algorithm 2, where the polytope is deformed by perturbing a single vertex and checking whether or not to discard the deformation immediately after. The next paragraph details the steps.

Algorithm 2 takes as its input the simplicial complex \mathcal{K} that triangulates the boundary of the initial convex polytope, the decay parameter α which controls the rate with which the volume of the set is increased or decreased while searching for the RFIS, and the maximum number of permissible subdivisions t_{max} . Since each iteration involves simplex subdivision, t_{max} bounds the maximum number of simplices in the simplicial complex that triangulates the boundary of the final polytopic set. The algorithm returns as output an ordered list of sets \mathcal{I} , for which the j -th entry $\mathcal{I}[j]$ is the simplicial complex that triangulates the boundary of the deformed polytope after j iterations of the algorithm. Line 1 of the algorithm initializes the values of the output set $\mathcal{I}[0]$.

The idea behind Algorithm 2 is to repeatedly perturb the vertices in a sequence until no vertex can be perturbed further, i.e. every vertex perturbation violates (34). Since this entails possibly perturbing a vertex more than once, we introduce an indicator Boolean variable $\text{IND}[j] \in \{0, 1\}$ that is 0 if the perturbation $\phi_j(v_j)$ in the previous iteration was discarded due to violating (34), and 1 otherwise. Since all vertices are initially candidates for being perturbed, line 3 initializes $\text{IND}[j] = 1 \forall j$. Consequently, each vertex is perturbed at least once through the vertex map ϕ_j as outlined in line 6. Whether or not a perturbation is successful in deforming the polytope is determined by computing (34). Since $\phi_j(v_j)$ induces a homeomorphism that only affects points in $\overline{\text{St}}_{\mathcal{K}}(v_j)$, it is sufficient to check for (34) over only the simplices in the closed star of the perturbed vertex. Therefore, lines 7-8 invoke Algorithm 1 to compute $\mathcal{N}(\Delta)$ - the ratio of test points that violate the **Boundary Condition** to the total

number of test points, for all the simplices in the closed stars of a vertex in \mathcal{K} (before perturbation) and in \mathcal{L} (after perturbation). Based on this, line 10 checks if (34) is true and lines 11-15 accordingly update the simplicial complex that triangulates the boundary of the polytope as follows: If a vertex deformation ϕ_j satisfies (34), then it is kept as shown in line 11, and the variable $\text{IND}[j]$ is set to 1 in line (12), indicating that further perturbation of vertices may be possible. If the vertex deformation must be discarded due to not satisfying (34), then the variable $\text{IND}[j]$ is set to 0 as shown in line (14). Note that the stop condition for the **while** loop is that $\text{IND}[j] = 0 \forall j$ (line 4), and that *all* vertices are perturbed even if $\text{IND}[j] = 1$ for only some j . This tends to avoid local minima, since perturbation of a vertex affects its entire closed star, and thus neighboring vertices that previously did not satisfy (34) may do so now upon perturbation. If (34) is still not satisfied, then the vertex deformation is discarded. This process is iterated until a stage is reached where all further perturbations violate (34), which causes the algorithm to exit the **while** loop. The resulting simplicial complex which triangulates the boundary of the deformed polytope is stored as $\mathcal{I}[t]$ for iteration t in line 18. Next, all simplices in the simplicial complex undergo barycentric subdivision as shown in line 19, and the vertex set of the simplicial complex is accordingly updated. This application of a sequence of vertex perturbations followed by a simplex subdivision is considered one iteration of the algorithm. The algorithm terminates when t_{\max} iterations are completed. Since any polytopic RFIS satisfies $\mathcal{N}(\Delta) = 0 \forall \Delta \in \mathcal{K}$, where \mathcal{K} triangulates the boundary of the polytopic RFIS, the algorithm checks whether the last simplicial complex $\mathcal{I}[t-1]$ triangulates the boundary of a polytopic RFIS in line 21.

In order to confirm that the generated polytopes are RFISs of different size, we can easily compute and track the volume enclosed by the polytope as the algorithm progresses, using only the simplicial complex that triangulates its boundary. This is also useful in proving that the algorithm terminates (Theorem V.2) and for benchmarking our results with existing work (Section VI). Although equation (8) only presents the formula to compute the volume of a simplex, it can be invoked to compute the volume of the polytope as follows. Since $\mathcal{I}[k]$ triangulates the boundary of a polytope for all k , we construct a triangulation for the polytope itself as follows: If $\Delta \in \mathcal{I}[k]$, then the set

$$\mathcal{I}'[k] = \left\{ \Delta' \mid \text{Vert}(\Delta') = \{c\} \cup \text{Vert}(\Delta), \forall \Delta \in \mathcal{I}[k] \right\}, \quad (35)$$

with $c \in \mathcal{R}_s$ triangulates the polytope. Thus, the volume enclosed by the polytope can be computed from the triangulation of its boundary, $\mathcal{I}[k]$, as

$$\text{Vol}(\mathcal{I}[k]) = \sum_{\Delta' \in \mathcal{I}'[k]} \text{Vol}(\Delta'), \quad (36)$$

where $\text{Vol}(\Delta')$ is computed using (8).

Theorem V.2. *Let \mathcal{K} be a simplicial complex that triangulates the boundary of a convex polytope containing \mathcal{R}_s for a nonlinear ℓ -Lipschitz continuous dynamical system F . Then, starting with $\mathcal{I}[0] = \mathcal{K}$ and parameter $\alpha \in (0, \infty)$, algorithm 2*

Algorithm 2: RFIS Computation Algorithm

Inputs : $\mathcal{K}, \alpha, F, \ell, m_{\max}, t_{\max}$
Outputs: \mathcal{I}

```

1 Set  $\mathcal{I}[0] = \mathcal{K}$ 
2 for  $t = 1, \dots, t_{\max}$  do
3   Initialize  $\text{IND}[j] = 1 \forall j \in \{1, \dots, N\}$  //  $N$  is
   //the cardinality of  $\text{Vert}(\mathcal{K})$ 
4   while  $\text{IND}[j] \neq 0 \forall j$  do
5     foreach  $j \in \{1, \dots, N\}$  do
6       Apply  $\phi_j : \text{Vert}(\mathcal{K}) \rightarrow \text{Vert}(\mathcal{L})$  on  $v_j$  // use (30)
7       foreach  $\Delta \in \overline{\text{St}}_{\mathcal{K}}(v_j) \cup \overline{\text{St}}_{\mathcal{L}}(v_j)$  do
8         Compute  $\mathcal{N}(\Delta) =$ 
           BCD_Test( $\text{Vert}(\Delta), F, \ell, m_{\max}$ )
9         end
10        if (34) is true then
11           $\mathcal{K} = \mathcal{L}$ 
12          Set  $\text{IND}[j] = 1$ 
13        else
14          Set  $\text{IND}[j] = 0$ 
15        end
16      end
17    end
18    Store  $\mathcal{I}[t] = \mathcal{K}$ 
19    Set  $\mathcal{K} = \mathbb{S}_B(\mathcal{K})$  // Barycentric subdivision
20  end
21  if  $\sum_{\Delta \in \mathcal{I}[t_{\max}]} \mathcal{N}(\Delta) \neq 0$  then
22    display "RFIS Not Found"
23  end
24  return  $\mathcal{I} = \{\mathcal{I}[0], \dots, \mathcal{I}[t_{\max}]\}$ 

```

terminates. Further, if $\mathcal{I}[k]$ is an RFIS for any iteration k , then the sequence $(\mathcal{I}[l])_{l \geq k}$ is a sequence of RFISs that successively reduce in volume if $\alpha < 1$, and increase in volume if $\alpha > 1$.

Proof. We show that the **while** loop (lines 4-17) terminates, i.e. the halting criterion $\text{IND}[j] = 0 \forall j$ is achieved in a finite number of iterations. Assume to the contrary that $\forall N \in \mathbb{N}, \exists k > N$ such that $\text{IND}[j] = 1$ for some j , in the k -th iteration of the **while** loop. Equivalently, (34) is true atleast once in every iteration. Because $\mathcal{N}(\Delta) \geq 0 \forall \Delta \in \mathcal{K}$, and because every strictly decreasing sequence of elements in a finite set converges to its least element, it follows that $\exists N$ such that $\mathcal{N}(\Delta) = 0 \forall \Delta \in \mathcal{K}$ and $\forall k > N$. In other words, \mathcal{K} triangulates the boundary of an RFIS for all $k > N$. Since the **while** loop continues indefinitely, there is atleast one j for which $\text{IND}[j] = 1$ infinitely often.

However, since $v_j \in \mathcal{B}_j(c) \forall j$ by definition, and since

$$\|\phi_j(v_j) - c\| \begin{cases} < \|v_j - c\|, & \alpha < 1 \\ > \|v_j - c\|, & \alpha > 1 \end{cases}, \quad (37)$$

where c was chosen to be in the interior of \mathcal{R}_s , it follows that ϕ_j maps v_j in the limit as $k \rightarrow \infty$ to either c or to ∞ along $\mathcal{B}_j(c)$, depending on whether $\alpha < 1$ or $\alpha > 1$ respectively. But, $v_j \in \text{Vert}(\mathcal{K})$ and \mathcal{K} triangulates the boundary of an RFIS $\forall k > N$. This contradicts $c \in \text{int}(\mathcal{R}_s)$ if $\alpha < 1$, and

$\text{Vol}(\mathcal{R}_m) < \infty$ if $\alpha > 1$. We conclude that the **while** loop terminates in finitely many iterations.

Next, we show that the sequence of sets generated due to the perturbations either increase or decrease monotonically in volume depending on the value of α . Let $\phi_j : \text{Vert}(\mathcal{K}) \rightarrow \text{Vert}(\mathcal{L})$, where \mathcal{K} and \mathcal{L} triangulate the boundaries of polytopes $\mathcal{P}_{\mathcal{K}}$ and $\mathcal{P}_{\mathcal{L}}$ respectively. We show that

$$\text{Vol}(\mathcal{P}_{\mathcal{L}}) \begin{cases} < \text{Vol}(\mathcal{P}_{\mathcal{K}}), & \alpha < 1 \\ > \text{Vol}(\mathcal{P}_{\mathcal{K}}), & \alpha > 1 \end{cases}. \quad (38)$$

The polytopes $\mathcal{P}_{\mathcal{K}}$ and $\mathcal{P}_{\mathcal{L}}$ are themselves triangulated by simplicial complexes \mathcal{K}' and \mathcal{L}' respectively, where these complexes are defined similar to (36). Then,

$$\begin{aligned} \text{Vol}(\mathcal{P}_{\mathcal{K}}) &= \sum_{\Delta \in \mathcal{K}'} \frac{1}{n!} \det(B_{\Delta}) \quad (39) \\ &= \sum_{\Delta \in \overline{\text{St}}_{\mathcal{K}'}(v_j)} \frac{1}{n!} \det(B_{\Delta}) + \sum_{\Delta \notin \overline{\text{St}}_{\mathcal{K}'}(v_j)} \frac{1}{n!} \det(B_{\Delta}) \quad (40) \end{aligned}$$

The second term in (40) is not affected by application of ϕ_j . However, for each simplex $\Delta \in \overline{\text{St}}_{\mathcal{K}'}(v_j)$, the volume after the perturbation is α times the volume before perturbation, as explained in what follows. Let $\text{Vert}(\Delta) = \{v_0, \dots, v_{n-1}, c\}$, so that

$$\text{Vol}(\Delta) = \frac{1}{n!} |\det [v_1 - v_0, \dots, v_{n-1} - v_0, c - v_0]| \quad (41)$$

$$= \frac{1}{n!} \left| \det \begin{bmatrix} v_0 & v_1 & \dots & v_{n-1} & c \\ 1 & 1 & \dots & 1 & 1 \end{bmatrix} \right| \quad (42)$$

Without loss of generality, consider the vertex map $\phi_0 : \text{Vert}(\mathcal{K}) \rightarrow \text{Vert}(\mathcal{L})$, and denote by Δ_0 the simplex after perturbation that corresponds to Δ . By definition of ϕ_0 , it follows that

$$\text{Vol}(\Delta_1) = \frac{1}{n!} \left| \det \begin{bmatrix} \alpha v_0 + (1-\alpha)c & \dots & v_{n-1} & c \\ 1 & \dots & 1 & 1 \end{bmatrix} \right|. \quad (43)$$

But the matrix in (43) can be obtained using elementary column transformations on the matrix in (42). Since multiplying a column by α multiplies the determinant by the same factor, it follows that $\text{Vol}(\Delta_0) = \alpha \text{Vol}(\Delta) \forall \Delta \in \overline{\text{St}}_{\mathcal{K}'}(v_j) \forall j$. Thus, each vertex map on the simplicial complex increases or decreases the volume of the polytope it triangulates, depending on whether $\alpha > 1$ or $\alpha < 1$ respectively. \square

Corollary V.2.1. *If the initial set $\mathcal{I}[0]$ is an RFIS, then $\mathcal{I}[k]$ is an RFIS for all k .*

Theorem V.2 suggests that if t_{\max} is sufficiently large, the sequence $(\mathcal{I}[k])$ will converge either to \mathcal{R}_s or \mathcal{R}_m respectively, depending on whether $\alpha < 1$ or $\alpha > 1$. However, the algorithm is greedy and may get stuck at a local minima if the deformations do not significantly change the volume enclosed by $\mathcal{I}[k]$. We simulate this for systems with known \mathcal{R}_s in two and three dimensions, and observe that when $\alpha < 1$, a good choice of initial polytope results in fast convergence to a polytopic approximation of \mathcal{R}_s , with t_{\max} as less as 6.

It is worth mentioning that the entire algorithm can be implemented knowing only $\text{Vert}(\Delta) \forall \Delta \in \mathcal{K}$. The quantities N_{Δ} , $\text{Vol}(\Delta)$ and \mathcal{T}_m are directly computed using the vertex

coordinates, and each vertex map replaces a row of L_{Δ} for each Δ that shares the vertex. Further, simplex subdivision simply replaces a given L_{Δ} with multiple such matrices, where the rows (vertices) are computed as outlined in [62].

VI. SIMULATIONS

This section presents the results of applying Algorithm 2 to various nonlinear dynamical systems. In all the figures, blue arrows and red curves represent the vector field and system trajectories respectively. The computation time for each iteration of the algorithm, and the volume enclosed by the resulting simplicial complex is presented in Table I. Section VI-A presents the simulation results for two-dimensional systems, and considers systems with and without additive disturbances. Further, Section VI-B presents the simulation results for three-dimensional systems. The algorithm terminates in an RFIS for each presented case, so that $\mathcal{N}(\Delta) = 0$ for all the simplices in the covering of the final polytope boundary. All computations were performed on a Dell Workstation with an Intel Xeon processor @ 3.30 GHz and 16 GB of RAM.

A. Two-State systems

1) *Van der Pol Oscillator:* The Van der Pol (VdP) oscillator is modeled by the system of equations:

$$\dot{x}_1 = x_2, \quad (44)$$

$$\dot{x}_2 = \mu(1 - x_1^2)x_2 - x_1, \quad (45)$$

where $x_1, x_2 : [0, \infty) \rightarrow \mathbb{R}$ are the states and the parameter μ indicates the strength of damping. The VdP oscillator has a stable limit cycle, which is also its minimal RFIS. Starting with a conservative initial polytopic invariant set with 6 vertices, $\mathcal{I}[0]$, and c as the origin, the results of Algorithm 2 with $\mu = 1$, $t_{\max} = 6$ are shown in Figs. 9 and 10 for $\alpha < 1$ and $\alpha > 1$ respectively. Clearly, $\alpha > 1$ corresponds to increasing the enclosed volume of the RFIS in every iteration. The more interesting application is when $\alpha < 1$, since the algorithm attempts to approximate the minimal RFIS, \mathcal{R}_s , and the result can be compared with the limit cycle of the VdP oscillator. The time taken for each iteration, along with the volume enclosed by $\mathcal{I}[k] \forall 0 \leq k \leq 6$ is shown in Table I. Note that $\mathcal{I}[k]$ is an RFIS $\forall k$.

2) *Fitzhugh-Nagumo Neuron Model:* The Fitzhugh-Nagumo system models the activity of an excitable system such as a neuron. For comparison, we use the same choice of parameters as [47], for which the system is modeled as:

$$\dot{x}_1 = x_1 - \frac{1}{3}x_1^3 - x_2 + \frac{7}{8}, \quad (46)$$

$$\dot{x}_2 = 0.08(x_1 + 0.7 - 0.8x_2). \quad (47)$$

We begin with an initial polytopic set (a convex quadrilateral) that is a conservative RFIS for the system. Setting $\alpha = 0.95$, $t_{\max} = 7$ and $c = [0 \ 1]^T$, it can be observed that Algorithm 2 converges to a polytopic approximation of \mathcal{R}_s , and there is no change in volume over the last iteration. Figure 11 shows a subset of the sequence of RFISs obtained using the algorithm. These polytopic approximations are much tighter than previous works such as Fig. 1 in [48] and Fig. 4 in [47].

Table I
COMPUTATION TIME AND ENCLOSED VOLUME AFTER EACH ITERATION FOR VARIOUS SYSTEMS

Iteration	Van der Pol (VdP)		Fitzhugh-Nagumo		Curve Tracking		Reversed VdP		Phytoplankton Growth		Thomas' Attractor	
	Time [s]	Volume	Time [s]	Volume	Time [s]	Volume	Time [s]	Volume	Time [s]	Volume	Time [s]	Volume
0		59.051		33		0.0431		0.3717		0.5827		8000
1	0.152	54.851	0.121	11.811	0.627	0.0431	6.55	0.1579	1.81	0.0028	1.404	371.22
2	0.281	31.104	0.122	10.051	0.679	0.0278	12.6	0.0681	8.65	0.0014	6.661	303.4
3	0.787	25.102	0.341	7.4795	1.319	0.0228	27.9	0.0373	271	0.0009	204.5	163.04
4	2.752	17.738	1.051	7.1519	3.725	0.0205	65.9	0.0347				
5	10.37	16.961	3.739	6.3052	12.07	0.0199	174	0.0347				
6	41.62	16.771	14.18	6.1651	42.67	0.0198						
7			56.02	6.1651	160.99	0.0198						

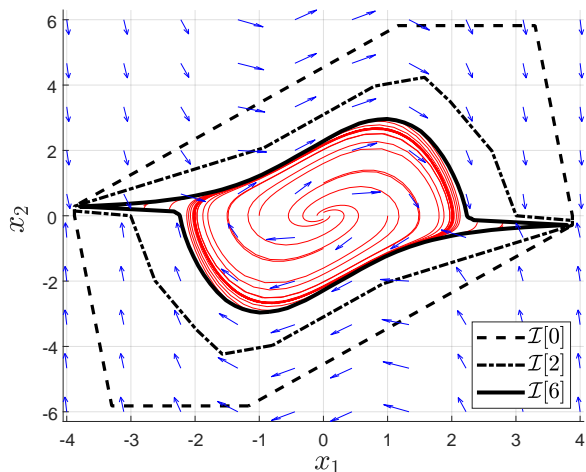


Figure 9. Van der Pol Oscillator, $\alpha = 0.98$.

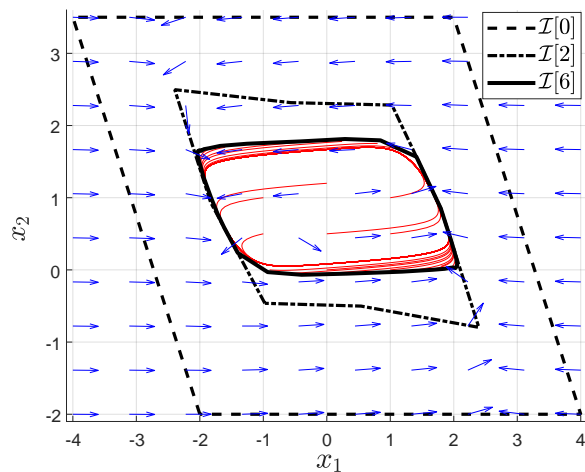


Figure 11. Fitzhugh-Nagumo Neuron Model

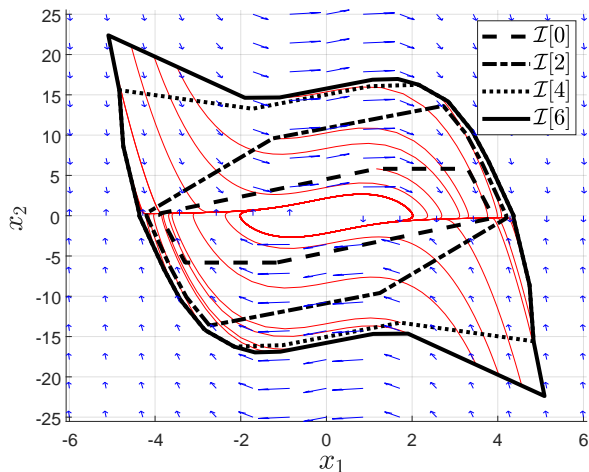


Figure 10. Van der Pol Oscillator, $\alpha = 1.02$.

3) *Curve Tracking Problem*: The curve tracking problem [69] is considered in the presence of disturbances, with $\omega = [\omega_1 \ \omega_2]^T : [0, \infty) \rightarrow \Omega$, with the noise space $\Omega = \{0\} \times [-1.5, 1.5] \subset \mathbb{R}^2$. The dynamics are modeled as:

$$\dot{x}_1 = -\sin(x_2) + \omega_1, \quad (48)$$

$$\dot{x}_2 = (x_1 - \rho) \cos(x_2) - \mu \sin(x_2) + \omega_2. \quad (49)$$

The results in Fig. 12 show the set valued map F with the extreme rays obtained by using $\omega_2(t) = \pm 0.15$. The blue cones in the figure represent the set of all directions in which the trajectory may move due to the disturbance. Some trajectories starting at the boundary of the obtained RFIS are also displayed, for a disturbance function of the form $\omega_1(t) = 0$, $\omega_2(t) = 0.15 \sin(t)$, with $\rho = 1$ and $\mu = 6.42$. For comparison, the noise function and system parameters are chosen to be the same as [57]–[59], where the minimal RFIS is computed using a different method. The agreement between the results confirms the validity of Algorithm 2, which converges in 6 iterations as evident from Table I.

4) *Reversed Van der Pol Oscillator*: The reversed Van der Pol oscillator is modeled by:

$$\dot{x}_1 = -x_2 + \omega_1, \quad (50)$$

$$\dot{x}_2 = x_1 - x_2 + x_2^3 + \omega_2. \quad (51)$$

We consider a polytopic noise space $\Omega = [-0.03, 0.03] \times [-0.03, 0.03]$. Figure 13 shows the set valued map F at different points in the state space, with the blue cones representing the set of directions that the trajectory may move depending on the disturbance. The values of \dot{x} obtained by using the vertices of Ω , $(\pm 0.03, \pm 0.03)$ are shown as vectors, in addition to three sets of system trajectories at a fixed set of initial points on the boundary of the RFIS obtained through the system. The first two sets of system trajectories

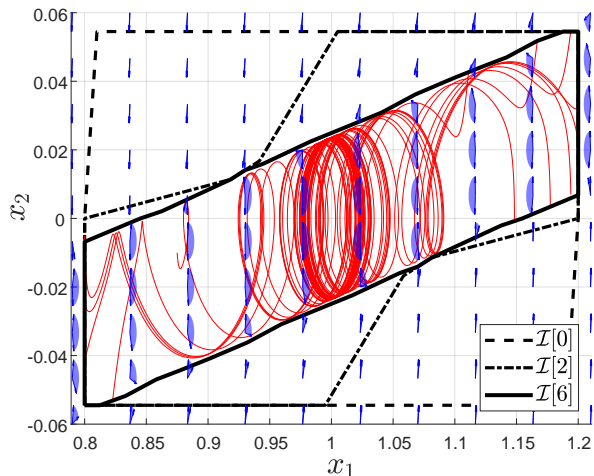


Figure 12. Curve Tracking Problem

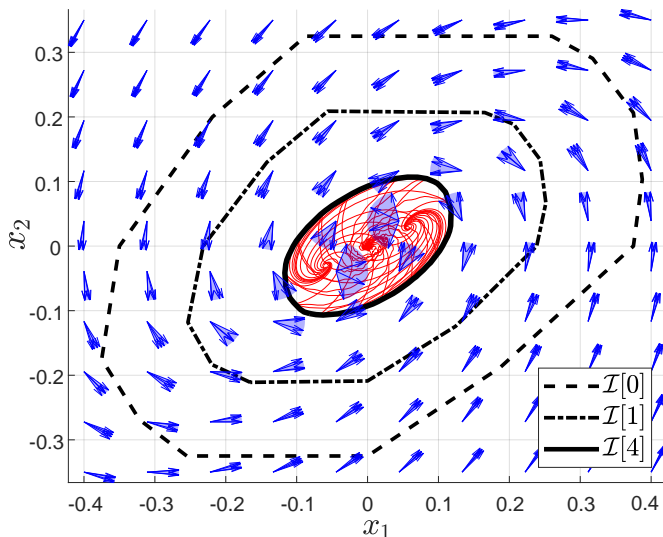


Figure 13. Reversed Van der Pol Oscillator

use constant disturbances $[\omega_1(t) \ \omega_2(t)]^T = [0.03 \ -0.03]^T$ and $[-0.03 \ 0.03]^T$ respectively, while the third set uses $\omega_1(t) = 0.01 \sin(2t) + 0.005 \sin(\pi t) + 0.015 \sin(6.53t)$, and $\omega_2(t) = -0.01 \cos(0.2t) + 0.02 \sin(5\pi t)$. Using $c = [0 \ 0]^T$ and $\alpha = 0.99$, Algorithm 2 converges in 4 iterations as evident from Table I.

B. Three-state systems

1) *Phytoplankton Growth Model*: Phytoplankton growth is modeled by the dynamical system:

$$\dot{x}_1 = 1 - x_1 - \frac{1}{4}x_1x_2, \quad (52)$$

$$\dot{x}_2 = (2x_3 - 1)x_2, \quad (53)$$

$$\dot{x}_3 = \frac{x_1}{4} - 2x_3^2. \quad (54)$$

The authors in [47] use optimization methods to obtain a conservative polytopic FIS for this model (see Fig. 5 in [47]).

Starting with an approximate recreation of this polytopic RFIS as $\mathcal{I}[0]$, and setting $c = [0.9969 \ 0.01 \ 0.3571]^T$, $\alpha = 0.9$, we obtain a much tighter approximation of \mathcal{R}_s for the system. In just 3 iterations of Algorithm 2, the polytope is deformed into a new polytopic RFIS, $\mathcal{I}[3]$ that is a much smaller RFIS than previous work, and encloses just 0.15% of the volume that $\mathcal{I}[0]$ did. Figure 14 shows the invariant sets $\mathcal{I}[0]$ and $\mathcal{I}[3]$, and Fig. 14(c) shows some system trajectories starting at the surface of the obtained RFIS. As expected, the trajectories move inward and never escape the RFIS.

2) *Thomas' Cyclically Symmetric Attractor*: Thomas' Attractor is described by the dynamical system:

$$\dot{x}_1 = \sin(x_2) - bx_1, \quad (55)$$

$$\dot{x}_2 = \sin(x_3) - bx_2, \quad (56)$$

$$\dot{x}_3 = \sin(x_1) - bx_3. \quad (57)$$

Here, b is a constant and acts as a bifurcation parameter. We consider $b = 0.3$, for which the system has two stable attractive limit cycles. Setting $\mathcal{I}[0]$ as a triangulation of the boundary of the cube with vertices $(\pm 10, \pm 10, \pm 10)$, the algorithm converges to an FIS in three iterations. The sets $\mathcal{I}[0]$ and $\mathcal{I}[3]$ are shown in Fig. 15, with Fig. 15(c) showing some system trajectories. Finally, when b is reduced to below ≈ 0.202816 , the limit cycle undergoes a period doubling cascade and becomes chaotic. We apply Algorithm 2 on the attractor when $b = 0.14$, and summarize the results in Fig. 16, where $\mathcal{I}[0]$, $\mathcal{I}[4]$ and some system trajectories are shown.

VII. FUTURE WORK AND CONCLUSION

A. Future Work

Our proposed approach opens new avenues for future research. In particular, a comprehensive study of vertex maps and the effect of their induced homeomorphisms on faster convergence of the algorithm would be interesting. For instance, vertex maps that map multiple vertices to different points, and adaptive adjustment of the parameters such as α and c , based on the behavior of the vector field at the boundary of the polytope is expected to speed up the algorithm. Further, if the homeomorphism is represented as a sequence of vertex maps as in our work, the algorithm may be further optimized by studying the ideal sequence in which to apply the maps, since homeomorphisms in general do not commute. The effect of simplex subdivision and the interplay between perturbing a vertex (through simplicial maps) and creating a vertex (through simplex subdivision) is another way to optimize the algorithm. Other measures of how close a simplex is to being invariant, besides $\mathcal{N}(\Delta)$, may also help aid this process. Thus, our algorithm can in fact be extended to a family of computational algorithms that search for an RFIS using (possibly variants of) the **Boundary Condition**. All such algorithms may be used on any Lipschitz continuous nonlinear dynamical system with bounded additive disturbances. Similar approaches may also be extended to compute control invariant sets for nonlinear systems.

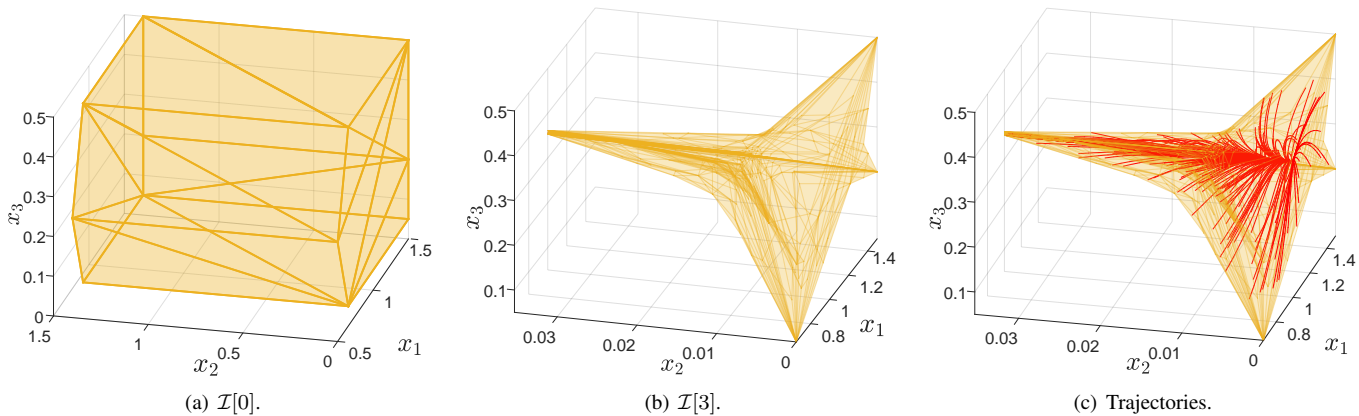
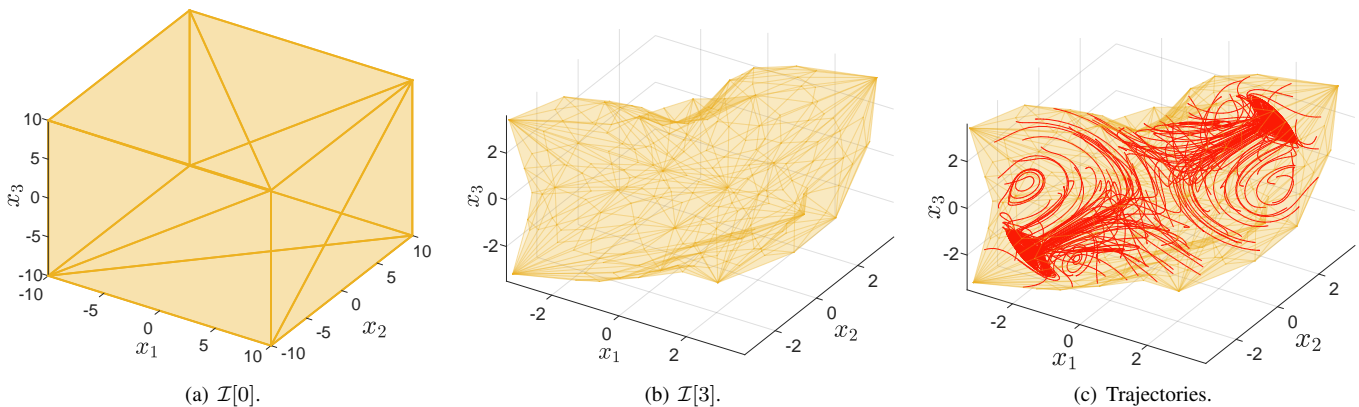


Figure 14. Phytoplankton Growth Model.

Figure 15. Thomas' Cyclically Symmetric Attractor, $b = 0.3$.

B. Conclusion

This paper developed an algorithm to generate a sequence of Robust Forward Invariant Sets of different sizes. First, we showed that if a nonlinear system's dynamics are Lipschitz continuous, then testing for invariance of a given (polytopic) set can be easily done by checking for a **Boundary Condition** on finitely many points, amounting to matrix-vector multiplication. Based on this, we developed an algorithm to deform a polytope into an RFIS, through a sequence of homeomorphisms induced by vertex maps on a simplicial complex that triangulates the boundary of the polytope. The geometric nature of the approach allows the algorithm to be used on any Lipschitz continuous nonlinear dynamical system in the presence of additive bounded disturbances. Application of the algorithm to a variety of nonlinear systems showed fast convergence and resulted in a sequence of RFIS of different sizes, that converged to approximate the minimal RFIS of the system.

APPENDIX

A. Proof of Lemma IV.6

We show that the linear transformation $T(M_m)$ from the standard simplex Λ to the simplex of interest Δ ensures that the reference test points on Λ map to points on Δ . Consider

$T(M_m) = M_m L_\Delta$, and let $x \in \mathcal{T}_m$, so that x is a row of $T(M_m)$ and thus a row combination of M_m and L_Δ . But the rows of L_Δ are just vertex coordinates of Δ , and each row of M_m is a lattice test point on Λ by construction. Further, $y \in \Lambda \implies \sum_{i=1}^n y_i = 1$. The matrix multiplication can be carried out as follows.

$$\begin{aligned}
 M_m L_\Delta &= \begin{bmatrix} M_{1,1} & M_{1,2} & \cdots & M_{1,n} \\ M_{2,1} & M_{2,2} & \cdots & M_{2,n} \\ \vdots & \vdots & \ddots & \vdots \\ M_{l_m,1} & M_{l_m,2} & \cdots & M_{l_m,n} \end{bmatrix} \begin{bmatrix} v_0^T \\ v_1^T \\ \vdots \\ v_{n-1}^T \end{bmatrix} \quad (58) \\
 &= \begin{bmatrix} \sum_{j=1}^n M_{1,j} v_{j-1}^T \\ \sum_{j=1}^n M_{2,j} v_{j-1}^T \\ \vdots \\ \sum_{j=1}^n M_{l_m,j} v_{j-1}^T \end{bmatrix} \quad (59)
 \end{aligned}$$

Since x is a row of this matrix, and since $0 \leq M_{i,j} \leq 1 \forall i, j$, and $\sum_{j=1}^n M_{i,j} = 1 \forall i$, it follows that x is a convex combination of the vertices of Δ , and hence, $x \in \Delta$. Since this is true for all $x \in \mathcal{T}_m$, we conclude that $\mathcal{T}_m \subset \Delta$.

B. Proof of Theorem IV.7

We now prove Theorem IV.7, which essentially says that testing for the **Boundary Condition** at a subset of test points

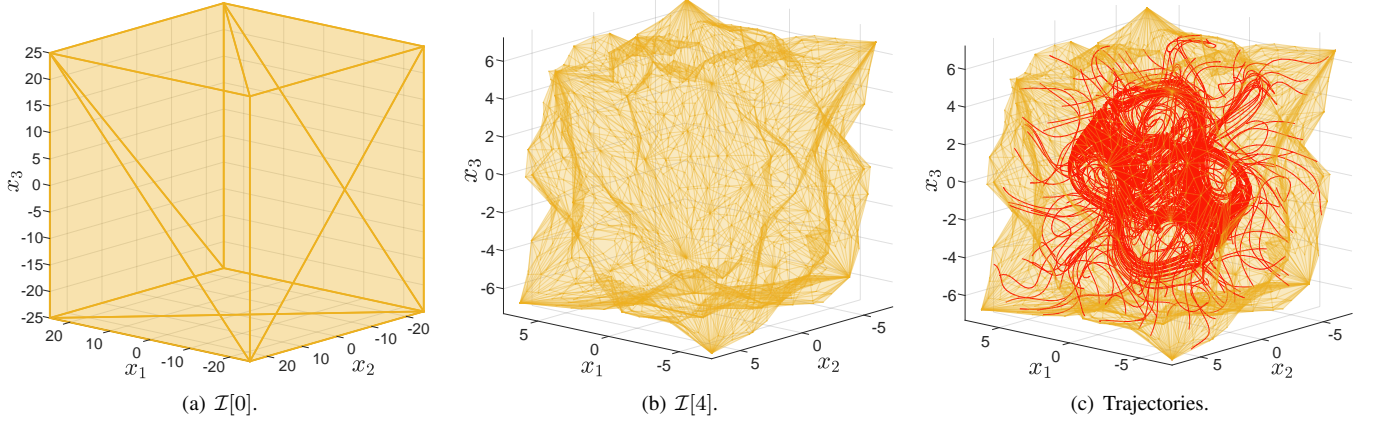
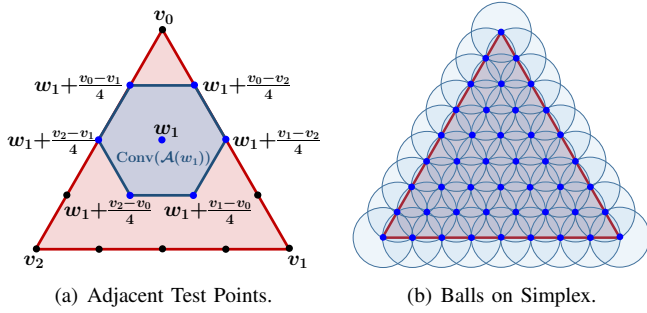
Figure 16. Thomas' Cyclically Symmetric Attractor, $b = 0.14$.

Figure 17. Simplex Proof Illustration.

is sufficient to check the invariance of the simplex. To establish this, we introduce the notion of adjacent lattice points.

Definition B.1 (Adjacent Lattice Point). *Let $w_1 \in \mathcal{T}_m \subset \Delta$ be a lattice test point. Another lattice point $w_2 \in \mathcal{T}_m$ is said to be adjacent to w_1 if $w_2 = w_1 \pm \delta_m(v_i - v_j)$, for any $v_i, v_j \in \text{Vert}(\Delta)$, where δ_m is defined in (22). If w is a lattice point, then $\mathcal{A}(w)$ denotes the set consisting of w and all its adjacent points.*

Adjacent points are easily visualized from Fig. 17(a), where the points in $\mathcal{A}(w_1)$ are colored blue. The convex hull of $\mathcal{A}(w_1)$ is shaded and denoted by $\text{Conv}(\mathcal{A}(w_1))$. Next, we show that these test points are appropriately spaced apart from each other. Specifically, there is a bound on the maximum distance a test point can be from all other test points.

Lemma B.2. *Let $r = \max_{i,j} \|v_i - v_j\|$, where $v_i, v_j \in \text{Vert}(\Delta)$. Further, let $w_i \in \mathcal{T}_m$ be any lattice test point. Then, $w_j \in \mathcal{A}(w_i) \implies \|w_i - w_j\| \leq r\delta_m$.*

Proof. Let $w_i \in \mathcal{T}_m$ be a lattice test point on Δ . Let $w_j \in \mathcal{A}(w_i)$ so that $w_j = w_i \pm \delta_m(v_i - v_j)$ by definition. Further, it follows for all w_j that

$$\|w_i - w_j\| = \delta_m \|v_i - v_j\| \quad (60)$$

$$\leq \delta_m \max_{i,j} \|v_i - v_j\| \quad (61)$$

$$\leq r\delta_m, \quad (62)$$

as desired. \square

Lemma B.2 shows that a ball of radius $r\delta_m$ around a given lattice test point always contains all adjacent lattice test points. This property of the test points allows us to propose the invariance test in Theorem IV.7, repeated here as Theorem B.3 for convenience.

Theorem B.3. *Let Δ be a given simplex with $\text{Vert}(\Delta) = \{v_0, \dots, v_{n-1}\}$, $r = \max_{i,j} \|v_i - v_j\|$, and \mathcal{T}_m be the set of test points on Δ for a given δ_m . Suppose that*

$$\langle F(x), N_\Delta \rangle \leq -r\delta_m \ell, \quad \forall x \in \mathcal{T}_m \quad (63)$$

where ℓ is the Lipschitz constant for the system dynamics given by F . Then, Δ is an invariant simplex.

Proof. Let $\mathcal{B}_k(z)$ represent the ball of radius k centered at z . We prove that if (63) is satisfied for all lattice test points, then every point on Δ satisfies the **Boundary Condition**.

From Lemma B.2, we know that $\mathcal{B}_{r\delta_m}(x)$ contains all adjacent lattice points. Thus, $\mathcal{A}(x) \subset \mathcal{B}_{r\delta_m}(x)$, and since $\mathcal{B}_{r\delta_m}(x)$ is a convex set, we also have $\text{Conv}(\mathcal{A}(x)) \subset \mathcal{B}_{r\delta_m}(x)$.

Taking the union over all lattice test points, we have

$$\bigcup_{x \in \mathcal{T}_m} \text{Conv}(\mathcal{A}(x)) \subset \bigcup_{x \in \mathcal{T}_m} \mathcal{B}_{r\delta_m}(x) \quad (64)$$

Since the vertices of the simplex are always lattice test points by construction, it follows that the left hand side of (64) is the simplex, Δ itself. Further, from Theorem IV.3, we know that the **Boundary Condition** is satisfied at all points in each of the balls, and therefore on all subsets of their union. Since Δ is one such subset, we conclude that Δ is an invariant simplex. \square

A visualization of this proof is provided in Fig. 17(b). The right hand side of (64) is the union of the balls on the simplex which contains the simplex itself.

REFERENCES

- [1] S. V. Raković, E. C. Kerrigan, K. I. Kouramas, and D. Q. Mayne, "Invariant approximations of the minimal robust positively invariant set," *IEEE Transactions on Automatic Control*, vol. 50, no. 3, pp. 406–410, 2005.
- [2] J. M. Bravo, D. Limón, T. Alamo, and E. F. Camacho, "On the computation of invariant sets for constrained nonlinear systems: An interval arithmetic approach," *Automatica*, vol. 41, no. 9, pp. 1583–1589, 2005.
- [3] D. Y. Rubin, H.-N. Nguyen, and P.-O. Gutman, "Computation of polyhedral positive invariant sets via linear matrix inequalities," in *Proceedings of the 2018 European Control Conference (ECC)*. IEEE, 2018, pp. 2941–2946.
- [4] M. Cannon, V. Deshmukh, and B. Kouvaritakis, "Nonlinear model predictive control with polytopic invariant sets," *Automatica*, vol. 39, no. 8, pp. 1487–1494, 2003.
- [5] K. Loparo and G. Blankenship, "Estimating the domain of attraction of nonlinear feedback systems," *IEEE Transactions on Automatic Control*, vol. 23, no. 4, pp. 602–608, 1978.
- [6] R. Genesio, M. Tartaglia, and A. Vicino, "On the estimation of asymptotic stability regions: State of the art and new proposals," *IEEE Transactions on Automatic Control*, vol. 30, no. 8, pp. 747–755, 1985.
- [7] F. Blanchini, "Set invariance in control," *Automatica*, vol. 35, no. 11, pp. 1747–1767, 1999.
- [8] E. Castelan and J. Hennet, "On invariant polyhedra of continuous-time linear systems," *IEEE Transactions on Automatic Control*, vol. 38, no. 11, pp. 1680–1685, 1993.
- [9] R. Ghaemi, J. Sun, and I. Kolmanovsky, "Less conservative robust control of constrained linear systems with bounded disturbances," in *Proceedings of the 47th IEEE Conference on Decision and Control (CDC)*. IEEE, 2008, pp. 983–988.
- [10] S. V. Raković and K. I. Kouramas, "Invariant approximations of the minimal robust positively invariant set via finite time Aumann integrals," in *Proceedings of the 46th IEEE Conference on Decision and Control (CDC)*. IEEE, 2007, pp. 194–199.
- [11] B. Rohal'-Ilkiv, "A note on calculation of polytopic-invariant feasible sets for linear continuous-time systems," *Annual Reviews in Control*, vol. 28, no. 1, pp. 59–64, 2004.
- [12] B. Pluymers, J. A. Rossiter, J. A. Suykens, and B. De Moor, "The efficient computation of polyhedral invariant sets for linear systems with polytopic uncertainty," in *Proceedings of the 2005 American Control Conference (ACC)*. IEEE, 2005, pp. 804–809.
- [13] T. B. Blanco, M. Cannon, and B. De Moor, "On efficient computation of low-complexity controlled invariant sets for uncertain linear systems," *International Journal of Control*, vol. 83, no. 7, pp. 1339–1346, 2010.
- [14] M. M. Seron, S. Oлару, F. Stoican, J. A. De Doná, and E. J. Kofman, "On finitely determined minimal robust positively invariant sets," in *Proceedings of the 2019 Australian & New Zealand Control Conference (ANZCC)*. IEEE, 2019, pp. 157–162.
- [15] A. Gupta, H. Köroğlu, and P. Falcone, "Computation of low-complexity control-invariant sets for systems with uncertain parameter dependence," *Automatica*, vol. 101, pp. 330–337, 2019.
- [16] C. Liu, F. Tahir, and I. M. Jaimoukha, "Full-complexity polytopic robust control invariant sets for uncertain linear discrete-time systems," *International Journal of Robust and Nonlinear Control*, vol. 29, no. 11, pp. 3587–3605, 2019.
- [17] T. Anevlavis and P. Tabuada, "Computing controlled invariant sets in two moves," in *Proceedings of the 58th IEEE Conference on Decision and Control (CDC)*. IEEE, 2019, pp. 6248–6254.
- [18] T. Anevlavis and P. Tabuada, "A simple hierarchy for computing controlled invariant sets," in *Proceedings of the 23rd International Conference on Hybrid Systems: Computation and Control*, 2020, pp. 1–11.
- [19] S. Yu, Y. Zhou, T. Qu, F. Xu, and Y. Ma, "Control invariant sets of linear systems with bounded disturbances," *International Journal of Control, Automation and Systems*, vol. 16, no. 2, pp. 622–629, 2018.
- [20] I. Kolmanovsky and E. G. Gilbert, "Theory and computation of disturbance invariant sets for discrete-time linear systems," *Mathematical Problems in Engineering*, vol. 4, no. 4, pp. 317–367, 1998.
- [21] F. Stoican, S. Oлару, J. A. De Doná, and M. M. Seron, "Zonotopic ultimate bounds for linear systems with bounded disturbances," *IFAC Proceedings Volumes*, vol. 44, no. 1, pp. 9224–9229, 2011.
- [22] F. Tahir and I. M. Jaimoukha, "Low-complexity polytopic invariant sets for linear systems subject to norm-bounded uncertainty," *IEEE Transactions on Automatic Control*, vol. 60, no. 5, pp. 1416–1421, 2014.
- [23] C.-J. Ong and E. G. Gilbert, "Outer approximations of the minimal disturbance invariant set," in *Proceedings of the 44th IEEE Conference on Decision and Control (CDC)*. IEEE, 2005, pp. 1678–1682.
- [24] C.-J. Ong and E. G. Gilbert, "The minimal disturbance invariant set: Outer approximations via its partial sums," *Automatica*, vol. 42, no. 9, pp. 1563–1568, 2006.
- [25] P. Trodden, "A one-step approach to computing a polytopic robust positively invariant set," *IEEE Transactions on Automatic Control*, vol. 61, no. 12, pp. 4100–4105, 2016.
- [26] S. V. Raković and M. Baric, "Parameterized robust control invariant sets for linear systems: Theoretical advances and computational remarks," *IEEE Transactions on Automatic Control*, vol. 55, no. 7, pp. 1599–1614, 2010.
- [27] M. Vašak, M. Baotić, and N. Perić, "Efficient computation of the one-step robust sets for piecewise affine systems with polytopic additive uncertainties," in *Proceedings of the 2007 European Control Conference (ECC)*. IEEE, 2007, pp. 1430–1435.
- [28] S. V. Raković, P. Grieder, M. Kvasnica, D. Q. Mayne, and M. Morari, "Computation of invariant sets for piecewise affine discrete time systems subject to bounded disturbances," in *Proceedings of the 43rd IEEE Conference on Decision and Control (CDC)*, vol. 2. IEEE, 2004, pp. 1418–1423.
- [29] T. Alamo, M. Fiacchini, A. Cepeda, D. Limon, J. M. Bravo, and E. F. Camacho, "On the computation of robust control invariant sets for piecewise affine systems," in *Assessment and Future Directions of Nonlinear Model Predictive Control*. Springer, 2007, pp. 131–139.
- [30] S. Dan and O. C. Jin, "Outer approximation of the minimal disturbance invariant set of pwl systems with bounded disturbances," in *Proceedings of the 9th International Conference on Control, Automation, Robotics and Vision*. IEEE, 2006, pp. 1–5.
- [31] S. Miani and C. Savorgnan, "MAXIS-G: A software package for computing polyhedral invariant sets for constrained LPV systems," in *Proceedings of the 44th IEEE Conference on Decision and Control (CDC)*. IEEE, 2005, pp. 7609–7614.
- [32] B. Pluymers, J. A. Rossiter, J. A. Suykens, and B. De Moor, "Interpolation based MPC for LPV systems using polyhedral invariant sets," in *Proceedings of the 2005 American Control Conference (ACC)*. IEEE, 2005, pp. 810–815.
- [33] E. Klintberg, M. Nilsson, A. Gupta, L. J. Mårdh, and P. Falcone, "Tree-structured polyhedral invariant set calculations," *IEEE Control Systems Letters*, vol. 4, no. 2, pp. 426–431, 2019.
- [34] J.-P. Aubin, *Viability theory*. Springer Science & Business Media, 2009.
- [35] M. Fiacchini, T. Alamo, and E. F. Camacho, "Invariant sets computation for convex difference inclusions systems," *Systems & Control Letters*, vol. 61, no. 8, pp. 819–826, 2012.
- [36] M. Fiacchini, S. Tarbouriech, and C. Prieur, "Polytopic control invariant sets for differential inclusion systems: a viability theory approach," in *Proceedings of the 2011 American Control Conference (ACC)*. IEEE, 2011, pp. 1218–1223.
- [37] K. I. Kouramas, S. V. Raković, E. C. Kerrigan, J. C. Allwright, and D. Q. Mayne, "On the minimal robust positively invariant set for linear difference inclusions," in *Proceedings of the 44th IEEE Conference on Decision and Control (CDC)*. IEEE, 2005, pp. 2296–2301.
- [38] S. V. Raković, K. I. Kouramas, E. C. Kerrigan, J. C. Allwright, and D. Q. Mayne, "The minimal robust positively invariant set for linear difference inclusions and its robust positively invariant approximations," *Automatica*, 2005.
- [39] Z. Artstein and S. V. Raković, "Feedback and invariance under uncertainty via set-iterates," *Automatica*, vol. 44, no. 2, pp. 520–525, 2008.
- [40] M. Fiacchini, T. Alamo, and E. F. Camacho, "On the computation of convex robust control invariant sets for nonlinear systems," *Automatica*, vol. 46, no. 8, pp. 1334–1338, 2010.
- [41] M. Fiacchini, T. Alamo, and E. F. Camacho, "On the computation of local invariant sets for nonlinear systems," in *Proceedings of the 46th IEEE Conference on Decision and Control (CDC)*. IEEE, 2007, pp. 3989–3994.
- [42] A. Iannelli, A. Marcos, and M. Lowenberg, "Estimating the region of attraction of uncertain systems with invariant sets," *IFAC-PapersOnLine*, vol. 51, no. 25, pp. 246–251, 2018.
- [43] D. Henrion and M. Korda, "Convex computation of the region of attraction of polynomial control systems," *IEEE Transactions on Automatic Control*, vol. 59, no. 2, pp. 297–312, 2013.
- [44] M. Korda, D. Henrion, and C. N. Jones, "Inner approximations of the region of attraction for polynomial dynamical systems," in *IFAC Symposium on Nonlinear Control Systems (NOLCOS)*, 2013, pp. 534–539.

- [45] G. Valmorbida and J. Anderson, "Region of attraction analysis via invariant sets," in *Proceedings of the 2014 American Control Conference (ACC)*. IEEE, 2014, pp. 3591–3596.
- [46] U. Topcu, A. K. Packard, P. Seiler, and G. J. Balas, "Robust region-of-attraction estimation," *IEEE Transactions on Automatic Control*, vol. 55, no. 1, pp. 137–142, 2009.
- [47] M. A. B. Sassi and A. Girard, "Computation of polytopic invariants for polynomial dynamical systems using linear programming," *Automatica*, vol. 48, no. 12, pp. 3114–3121, 2012.
- [48] M. A. B. Sassi, A. Girard, and S. Sankaranarayanan, "Iterative computation of polyhedral invariants sets for polynomial dynamical systems," in *Proceedings of the 53rd IEEE Conference on Decision and Control (CDC)*. IEEE, 2014, pp. 6348–6353.
- [49] M. Lazar, A. Alessio, A. Bemporad, and W. Heemels, "Squaring the circle: An algorithm for generating polyhedral invariant sets from ellipsoidal ones," in *Proceedings of the 2006 American Control Conference (ACC)*. IEEE, 2006, pp. 3007–3012.
- [50] S. V. Raković and M. Fiacchini, "Invariant approximations of the maximal invariant set or "encircling the square"," *IFAC Proceedings Volumes*, vol. 41, no. 2, pp. 6377–6382, 2008.
- [51] A. Alessio, M. Lazar, A. Bemporad, and W. Heemels, "Squaring the circle: An algorithm for generating polyhedral invariant sets from ellipsoidal ones," *Automatica*, vol. 43, no. 12, pp. 2096–2103, 2007.
- [52] R. Schreier, M. V. Goodson, and B. Zhang, "An algorithm for computing convex positively invariant sets for delta-sigma modulators," *IEEE Transactions on Circuits and Systems I: Fundamental Theory and Applications*, vol. 44, no. 1, pp. 38–44, 1997.
- [53] T. B. Blanco and B. De Moor, "Polytopic invariant sets for continuous-time systems," in *Proceedings of the 2007 European Control Conference (ECC)*. IEEE, 2007, pp. 5087–5093.
- [54] R. M. Schaich and M. Cannon, "Robust positively invariant sets for state dependent and scaled disturbances," in *Proceedings of the 54th IEEE Conference on Decision and Control (CDC)*. IEEE, 2015, pp. 7560–7565.
- [55] A. Chakrabarty, A. Raghunathan, S. Di Cairano, and C. Danielson, "Data-driven estimation of backward reachable and invariant sets for unmodeled systems via active learning," in *Proceedings of the 57th IEEE Conference on Decision and Control (CDC)*. IEEE, 2018, pp. 372–377.
- [56] Y. Chen, H. Peng, J. Grizzle, and N. Ozay, "Data-driven computation of minimal robust control invariant set," in *Proceedings of the 57th IEEE Conference on Decision and Control (CDC)*. IEEE, 2018, pp. 4052–4058.
- [57] S. Mukhopadhyay, "Robust forward invariant sets for nonlinear systems," Ph.D. dissertation, Georgia Institute of Technology, 2014.
- [58] S. Mukhopadhyay and F. Zhang, "A path planning approach to compute the smallest robust forward invariant sets," in *Proceedings of the 2014 American Control Conference (ACC)*. IEEE, 2014, pp. 1845–1850.
- [59] S. Mukhopadhyay and F. Zhang, "An algorithm for computing robust forward invariant sets of two dimensional nonlinear systems," *Asian Journal of Control*, 2020.
- [60] P. Varnell, S. Mukhopadhyay, and F. Zhang, "Discretized boundary methods for computing smallest forward invariant sets," in *Proceedings of the 55th IEEE Conference on Decision and Control (CDC)*. IEEE, 2016, pp. 6518–6524.
- [61] P. Varnell and F. Zhang, "Computing largest tolerable disturbance sets," in *Proceedings of the 2018 American Control Conference (ACC)*. IEEE, 2018, pp. 6114–6119.
- [62] H. Edelsbrunner and J. Harer, *Computational topology: an introduction*. American Mathematical Soc., 2010.
- [63] H. K. Khalil, *Nonlinear systems; 3rd ed.* Upper Saddle River, NJ: Prentice Hall, 2002.
- [64] J.-P. Aubin and A. Cellina, *Differential inclusions: set-valued maps and viability theory*. Springer Science & Business Media, 2012, vol. 264.
- [65] S. Boyd and L. Vandenberghe, *Convex optimization*. Cambridge University Press, 2004.
- [66] G. E. Bredon, *Topology and geometry*. Springer Science & Business Media, 2013, vol. 139.
- [67] J. Lee, *Introduction to topological manifolds*. Springer Science & Business Media, 2010, vol. 202.
- [68] J. W. Gorman and J. E. Hinman, "Simplex lattice designs for multicomponent systems," *Technometrics*, vol. 4, no. 4, pp. 463–487, 1962.
- [69] M. Malisoff, F. Mazenc, and F. Zhang, "Stability and robustness analysis for curve tracking control using input-to-state stability," *IEEE Transactions on Automatic Control*, vol. 57, no. 5, pp. 1320–1326, 2011.